mtDNA recombination indicative of hybridization suggests a role of the mitogenome in the adaptation of reef-building corals to extreme environments

Eulalia Banguera-Hinestroza[1,2], Yvonne Sawall[3], Abdulmohsin Al-Sofyani[4], Patrick Mardulyn[2], Javier Fuertes-Aguilar[5], Heiber Cárdenas-Henao[6], Francy Jimenez-Infante[1], Christian R. Voolstra[1**], Jean-François Flot [2**]*

1. Red Sea Research Center, King Abdullah University of Sciences and Technology (KAUST), Thuwal, Saudi Arabia.
2. Ecology and Evolutionary Biology, Université libre de Bruxelles (ULB), Brussels. Belgium.
3. Bermuda Institute of Ocean Sciences (BIOS), Coral Reef Ecology, Bermuda.
4. Department of Marine Biology, Faculty of Marine Sciences, King Abdulaziz University (KAU), Jeddah, Saudi Arabia.
5. Real Jardín Botánico, RJB-CSIC, Plaza de Murillo 2, 28014 Madrid, Spain.
6. Universidad del Valle, Department of Biology. Group of Ecogenetics and Molecular Biology, Cali, Colombia.

*Corresponding author:
Eulalia Banguera-Hinestroza, ebanguer@ulb.ac.be; eulalia.banguera@gmail.com
** Equal contributions

Abstract

mtDNA recombination following hybridization is rarely found in animals and was never until now reported in reef-building corals. Here we report unexpected topological incongruence among mitochondrial markers as evidence of mitochondrial introgression in the phylogenetic history of *Stylophora* species distributed along broad geographic ranges. Our analyses include specimens from the Indo-Pacific, the Indian Ocean and the full latitudinal (2000 km) and environmental gradient (21°C-33°C) of the Red Sea (N=827). The analysis of *Stylophora* lineages in the framework of the mitogenome phylogenies of the family Pocilloporidae, coupled with analyses of recombination, shows the first evidence of asymmetric patterns of introgressive hybridization associated to mitochondrial recombination in this genus. Hybridization likely occurred between an ancestral lineage restricted to the Red Sea/Gulf of Aden basins and migrants from the Indo-Pacific/Indian Ocean that reached the Gulf of Aden. The resulting hybrid lives in sympatry with the descendants of the parental Red Sea lineage, from which it inherited most of its mtDNA (except a highly variable recombinant region that includes the *nd6*, *atp6*, and mt*ORF* genes) and expanded its range into the hottest region of the Arabian Gulf, where it is scarcely found. Noticeably, across the Red Sea both lineages exhibit striking differences in terms of phylogeographic patterns, clades-morphospecies association, and zooxanthellae composition. Our data suggest that the early colonization of the Red Sea by the ancestral lineage, which involved overcoming multiple habitat changes and extreme temperatures, resulted in changes in mitochondrial proteins, which led to its successful adaptation to the novel environmental conditions.

Key words: Introgressive hybridization, coral reefs, extreme environments, mtDNA recombination, mito-mito incongruence, mito-nuclear incongruence, *Stylophora*, Pocilloporidae, Red Sea.

1. INTRODUCTION

Studies of mitochondrial genomes have been of broad relevance for understanding the ecological and evolutionary processes leading to the diversification of organisms (Ballard and Rand 2005; Chinnery and Hudson 2013; Kivisild 2015; Wolff et al. 2016), due particularly to key characteristics such as: maternal inheritance (in most organisms); high mutation rates in triploblastic metazoans (but not in cnidarians and poriferans; cf. Shearer et al. 2002); and lack of recombination (Barr et al. 2005). However, the latter assumption has been challenged by the increasing evidence of mtDNA recombination in animals (Rokas et al. 2003; Barr et al. 2005; Tsaousis et al. 2005; Ujvari et al. 2007; Ladoukakis and Zouros 2017) with important ecological and evolutionary implications (Rokas et al. 2003; White et al. 2008; Dokianakis and Ladoukakis 2014; Levsen et al. 2016).

In natural populations, most evidence for mtDNA and/or nuclear introgression comes from species living at the edge of their geographic range (i.e. marginal ecosystem that often exhibit genetically atypical populations; Johannesson and André, 2006), perturbed habitats, near extreme environmental conditions or in hybrid zones (Riginos and Cunningham 2004; Johannesson and Carl 2006; Brennan et al. 2014; Taylor et al. 2015; Hellberg et al. 2016). There is growing evidence in plants, in fungi, and to a lesser extent in animals, that divergent lineages that meet and interbreed in contact zones, particularly after expanding their range as a consequence of climatic or habitat fluctuations, produce hybrids carrying recombinant mitochondrial genomes (Barr et al. 2005) that are able to adapt to new environmental or habitat conditions leading eventually to hybrid speciation (Riginos and Cunningham 2004; Brennan et al. 2014; Taylor et al. 2015; Mastrantonio et al. 2016).

Marginal areas such as the Red Sea, a biogeographic *cul-de-sac* extending from the Indian Ocean, are observed to host a high number of hybrid species (Veron 1995; Johannesson and Carl 2006; DiBattista et al. 2016; Berumen et al. 2017) and therefore offer an interesting playground to study the main factors influencing patterns of diversification and speciation in extreme environments. This basin exhibits a high variability in oceanographic conditions following a N-S gradient along four well-defined oceanographic provinces (Raitsos et al. 2013), ranging from

relatively low temperatures in the northern areas (below 23°C) to record summer temperatures up to 33°C in the southern regions (Acker et al. 2008; Raitsos et al. 2013; Moustafa et al. 2014; Sawall et al. 2014; Sawall et al. 2015).

In addition, since its inception this region has undergone a complex climatic and geological history. During the last glacial cycles, the Red Sea experienced multiple sea-level fluctuations (Siddall et al. 2003; Rohling et al. 2013) as well as repetitive periods of connection and isolation from the Indo-Pacific, through the Strait of Bab-el-Mandeb in the South (Righton et al. 1996; Siddall et al. 2004; Rohling et al. 2013). These events, together with discontinuous periods of extinction and re-colonization from refuge zones inside and outside the region (Fine et al. 2013; Pellissier et al. 2014), likely played an important role in shaping the geographic distribution of genetic diversity for coral reefs in this oceanic basin, as well as the diversification of their associated fauna (DiBattista et al. 2013; DiBattista et al. 2016a; DiBattista et al. 2016b; Berumen et al. 2017). In fact, it has been postulated that corals entered the region during the Miocene –a period characterized by hyper-saline conditions and strong climate change– and after several episodes of post-Miocene migrations (Taviani 1998). Therefore, lineages already inhabiting this area were affected by the successive geological and climatic processes influencing the region (DiBattista et al. 2016). Repetitive invasions from the Indian Ocean likely enhanced the potential for the encounter of lineages with different genetic backgrounds, increasing the chance for hybridization and therefore hybrid speciation in the unique conditions of this marine zone.

Introgressive hybridization has been reported to be widespread in reef-building corals, with records mostly in the families Acroporidae, Poritidae and Pocilloporidae (Van Oppen et al. 2001; Willis et al. 2006; Combosch and Vollmer 2015; Richards and Hobbs 2015; Hellberg et al. 2016; Forsman et al. 2017; Johnston et al. 2017). Indeed, the topological incongruence observed in coral phylogenies might be explained by reticulate evolution due to multiple climatic and see-level changes across geological eras (Veron 1995; Van Oppen et al. 2001; Vollmer and Palumbi 2002; Willis et al. 2006). Moreover, it has been proposed that many species occurring in marginal areas and with restricted distribution, such as those endemic of the Indo-Pacific Ocean, might be hybrids (Veron 1995; Richards and Hobbs 2015). Even though mtDNA introgression is

110 expected to be more frequent than nuclear introgression, particularly between species occurring
111 in sympatry (Mastrantonio et al. 2016), it has not being reported to date in reef-building corals.
112
113 The coral genus *Stylophora* (family Pocilloporidae) is widely distributed in the Indo-Pacific and
114 Indian Ocean and comprises a range of a highly plastic morphospecies (Veron 1995; Veron
115 2002), which are diversified within four phylogenetic lineages (Flot et al. 2011; Stefani et al.
116 2011; Keshavmurthy et al. 2013). *Stylophora* is found throughout the entire environmental range
117 of the Red Sea and is represented by several morphospecies: *Stylophora pistillata* (Esper, 1797),
118 *Stylophora subseriata* (Ehrenberg, 1834), *Stylophora wellsi* (also found in Madagascar),
119 *Stylophora kuelhmanni*, *Stylophora danae* and *Stylophora mamillata* (Scheer and Pillai 1983;
120 Veron 2002). A recent molecular study aiming to identify species boundaries in the genus
121 (Arrigoni et al. 2016) proposes that all these morphospecies belong to one single cohesive
122 molecular lineage.
123
124 We selected the genus *Stylophora* given its widespread geographical distribution and the
125 presence of several endemic morphospecies in the Red Sea (Veron et al. 2018), which may
126 represent important sources of genetic variability for the future adaptation of reef-building corals
127 under the current threats of climate changes. Coral species within this genus and their associated
128 zooxanthellae were studied across the environmental gradients of the Red Sea, spanning over
129 ~2000Km (12 degrees of latitude) and sequences from other relevant biogeographic regions were
130 also included (i.e. New Caledonia, Great Barrier Reef, Madagascar, Gulf of Aden and Arabian
131 Gulf). A total of 827 sequences were analyzed to understand their genetic diversity, phylogenetic
132 history and phylogeographic framework, in addition 281 colonies were typified for
133 *Symbiodinium.*
134
135 Our study was centered in mtDNA genes, but nuclear markers were included to understand
136 differences in phylogenetic and phylogeographic patterns. Molecular analyses included ITS2 for
137 *Symbiodinium* and four nuclear (*hsp70*, ITS1, ITS2 and *PMCA*) and five mitochondrial genes for
138 the coral host (mtCR, *cox1*, 12S, 16S and *atp6*-mt*ORF*). Subsequently, the patterns of
139 diversification of the Red Sea specimens, outlined by mtDNA genes, were evaluated using full

140 mitochondrial genome sequences of species belonging to the family Pocilloporidae (*Pocillopora*,
141 *Seriatopora*, *Stylophora* and *Madracis*) (Veron and Pichon 1976).
142
143 Our aims were (1) to investigate patterns of diversification in *Stylophora* species along broad
144 geographic ranges and verified further whether host morphological variation had any taxonomic
145 value for Red Sea species (in other words, is there any association between morphological and
146 genetic variation?). (2) to find out whether mitochondrial variation, zooxanthellae association, and
147 phylogeographic patterns fit the trends expected from the environmental gradients in this marginal
148 basin, and (3) to test whether the topological incongruence between mtDNA markers observed in
149 our data and previously reported by Arrigoni et al. (2016) could be explained by introgressive
150 hybridization. Here we discuss our results from an integrative perspective, coupling phylogenetic
151 and phylogeographic patterns, *Symbiodinium* distribution, morphospecies-clades association and
152 the finding of mtDNA recombination. We also discuss the implications of these results for coral
153 conservation in highly variable environments.
154
155 **2. RESULTS**
156
157 **2.1. Gene variation and polymorphic sites**
158
159 Our largest data set consisted of 827 sequences of the mt*ORF* locus, which includes a short
160 region of the adjacent *atp6* gene, from a large portion of the geographic distribution of
161 *Stylophora* (Figure 1, Supplementary Table *S1*); it included 716 samples from our collection of
162 the Red Sea, 3 samples from the Arabian Gulf, plus 108 sequences of *S. pistillata* morphospecies
163 from Stefani et al. (2011) and Flot et al. (2011): from the Gulf of Aden (N=20), Pacific regions
164 (N=60) and Madagascar (N=28). In addition, we produced a second dataset for four other
165 mitochondrial fragments, from CR (N=401), *cox1* (N=147), 12S (N=72) and 16S (N=61) and
166 four nuclear fragments, from *hsp70* (N=738), ITS1 (N=75), ITS2 (N=56) and *PMCA* (N=86)
167 genes. This data set includes sequences from other studies (see material and methods section 4).
168
169 While the *atp6*-mt*ORF* locus (N=827; 884-943 bp) displayed a high level of polymorphism in
170 *Stylophora* samples, the two *cox1* fragments (303-545 bp) were found monomorphic when

comparing sequences across all Red Sea specimens. Pairwise comparisons among all individuals uncovered multiple synonymous and non-synonymous substitutions at the 5' end and 3' end of the mt*ORF* gene, but noticeably, the core region was composed mainly by duplicated tandem repeats, which were of variable lengths and dissimilar among *Stylophora* specimens from the Red Sea (in terms of nucleotide composition and length of the repeat; data not shown).

In addition, the analysis of the full *atp6* sequences revealed a high number of mutations in this gene. Two haplotypes were found among Red Sea specimens differing by 50 point mutations, which were differentiated from an Indo-Pacific/Indian Ocean haplotype in 45 and 8 point mutations respectively. Most changes at the *atp6* gene were synonymous, except two changes found at positions 104 (i.e. Asparagine –AAT– / Valine –GTT– / Isoleucine –ATT–) and at position 187 (Serine –TCA–/Phenylalanine –TTT–/ Leucine –TTA–) resulting in changes that involved amino acid with different polarities.

The CR (N=401; 757 bp) was the most variable of the non-coding markers, with polymorphism mainly caused by variation in the number of tandem repeats, some of them being specific to *Stylophora* specimens inhabiting different geographic areas. Polymorphic sites, indels and parsimony informative sites for mitochondrial and nuclear genes are recorded in Supplementary Table *S2*.

2.2. Phylogenetic analyses

ML and Bayesian phylogenies inferred from the *atp6*-mt*ORF* locus including *Pocillopora* as an outgroup (no shown) or excluding the outgroup (Figure 2a) showed a large phylogenetic subdivision between two groups, each associated with both high Bayesian Posterior Probabilities (BPP > 1.0) and high bootstrap values (> 99%). A first clade, (N=461; h=27) included some of the sequences from the Red Sea and the Gulf of Aden and those from the Arabian Gulf (N=373; h=12), plus sequences from Madagascar (N=28, h=6) and the Pacific (N=60; h=9); the second clade included the other specimens from the Red Sea and Gulf of Aden (N=366; h=14) –we refer to this clade as the Red Sea Lineage B (*RS_LinB*)– (Figure 2a). These two lineages were also evident in the mitogenome phylogenies of the family using the full *atp6* (678 bp) and *nd6* genes

202 (564 bp) (Figure 3a) and in the phylogenies derived from our recombination analyses (Figure 3b)
203 –See recombination results below–.

204 In contrast, in the phylogenetic trees inferred from all other markers, whether mitochondrial (CR,
205 12S) or nuclear (ITS1; ITS2*, hsp70; PMCA*) (Figures 2b and Supplementary Figure *S1*),
206 *RS_LinA* and *RS_LinB* sequences form a clade that exclude all sequences from Madagascar and
207 from the Indo-Pacific region. There is therefore a major incongruence between the phylogenetic
208 signal of *atp6*, *nd6* and the mt*ORF* vs the CR and 12S (Figure 2 and Figure 3a) and between
209 mtDNA genes vs the nuclear genes. The ITS2 showed a pattern similar to that of the CR, in
210 which *RS_LinA* and *RS_LinB* are almost completely separated; there is only one individual from
211 *RS_LinB* placed inside the clade formed by *RS_LinA* sequences, and vice versa, on the ITS2 tree
212 (Supplementary Figure *S1*). The *cox1* and the 16S trees provided only little phylogenetic
213 information (not shown).
214
215 **2.3. Comparative analyses between *RS_LinA* and *RS_LinB***
216
217 **2.3.1. Intraspecific phylogenies and morphospecies-clade association**
218
219 Bayesian and ML trees obtained based on the full-length sequences of the *atp6*-mt*ORF* locus,
220 thus analyzing members of each lineage (*RS_LinA,* 884 bp, h=33; *RS_LinB*, 943 bp, h=20)
221 separately, are shown in Figure 4. In general, we found no clear association between Red Sea
222 morphospecies and phylogenetic groups in the *RS_LinA* lineage. For example, some
223 mitochondrial haplotypes were shared among different morphotypes or/and individuals
224 exhibiting the same morphotypes were placed into different subclades (Figure 4a); the only
225 exceptions were haplotypes belonging to morphotypes of *S. kuelhmanni*, that were all associated
226 with subclade *LA1*, and those from *S. mamillata* –from Arrigoni et al. (2016)– that were
227 exclusively found in subclade *LA3* (data not shown). Instead, in the *RS_LinB* lineage,
228 morphotypes attributed to *S. subseriata* (called *Stylophora* cf. *subseriata* thereafter) were
229 grouped in subclade *LB1* and displayed haplotypes found exclusively in the northern Red Sea –
230 see phylogeographic analyses below– and were differentiated from morphotypes belonging to *S.*
231 *pistillata* (mainly short and medium branched morphotypes, called as *Stylophora* cf. *pistillata*
232 from now on), whose haplotypes were distributed mainly in the central-southern Red Sea and
233 were placed in subclade *LB2* (Figure 4b).

234 **2.3.2. *Symbiodinium* distribution**

235

236 As for zooxanthellae, *Symbiodinium* type A1 (*Symbiodinium microadriaticum*) was the most
237 abundant in members of *Stylophora* within the Red Sea (167 out of 281 colonies), followed by
238 *Symbiodinium* type C160 (N=49). The distribution of these types was somehow different
239 between members of each *Stylophora* mtDNA lineage (Figure 4). In colonies placed within the
240 *RS_LinB* and inhabiting the northern Red Sea (i.e. subclade *LB1*; *Stylophora* cf. *subseriata*;
241 N=76) the most abundant type was C160 (N=41) followed by type A1 (N=22) and few colonies
242 presented both types (A1-C160; N=9). In contrast, colonies distributed in the central-southern
243 areas (i.e. subclade *LB2*; i.e. *Stylophora* cf. *pistillata*) were mainly associated with type A1 (40
244 out of 54 colonies) and the presence of C160 type, or of this type in combination with A1 (A1-
245 C160) were not detected. In southern regions, few colonies exhibited the C1* type, which was
246 not present in northern colonies and was always found in association of type A1 (i.e. A1-C1*;
247 N=10). Other C types or associations A1-C types were found in very low abundance (i.e. in one
248 colony). A high percentage of the colonies of the *Stylophora RS_LinA* (105 colonies out of 151)
249 showed association with *Symbiodinium microadriaticum* in both northern and southern regions.
250 The few colonies carrying C160 or A1-C160 types were mainly found in Yanbu (7 out of 11
251 colonies). The presence of C1* and A1-C1* types were detected mostly in colonies inhabiting
252 the southernmost area of the Red Sea (i.e. Farasan; 7 out of 8 colonies). Few C types (i.e. C161,
253 C162, C116) and combination of A1 with other types (i.e. A1-D, A1-C41, A1-B, A1-C1, A1-
254 C19; A1-sp) displayed low frequencies and some of them were exclusive of colonies belonging
255 to this group (Figure 4).

256

257 **2.4. Comparative phylogeography of *RS_LinA* and *RS_LinB* and patterns of genetic**
258 **variation along the Red Sea gradient**

259

260 Median-joining networks were constructed for the markers for which we had the largest number
261 of sequences: *atp6*-mt*ORF* (N=827), CR (N=401) and *hsp70* (N=738). Each network indicates a
262 clear phylogeographic signal (i.e., there was a visible association between genetic variation and
263 geographic location). The north-south genetic differentiation was more pronounced for *RS_LinB*
264 than for *RS_LinA*, a pattern supported by all three loci (Figure 5). Haplotype frequencies along

265 the gradient were somehow different among lineages. In *RS_LinB* the highest frequencies of the
266 most common haplotypes were found either in northern or southern areas, while haplotype
267 frequencies in *RS_LinA* showed a clinal variation (Supplementary Figure *S2*). For the *hsp70*,
268 haplotypes showed different frequencies along the gradient when evaluated per mtDNA lineage
269 (Supplementary Figure *S2c*) and the pattern was similar to that shown by the *atp6*-mt*ORF* locus.
270
271 **2.5. mtDNA recombination analyses**
272
273 The analyses of the mitogenomes for all members of the family Pocilloporidae including
274 *RS_LinA* and *RS_LinB* and the genus *Polycyathus*, resulted in the detection of several
275 recombination events in pocilloporid corals. Recombination signals were detected in *Stylophora,*
276 *Seriatopora and Madracis.* The signals for *Stylophora* and *Seriatopora* were confirmed when
277 excluding the two divergent genomes of *Madraci*s and *Polycyathus*. In *Stylophora* the strongest
278 signal supported by all seven methods was found in *RS_LinA*, with the major parent
279 hypothesized as the *RS_LinB* and the minor parent *Stylophora pistillata* (Taiwan). *P*-values were
280 as follow: RDP = 1.175 x 10^{-10}; GENECONV = 8.96 x 10^{-11}; BOOTSCAN = 1.237 x 10^{-11};
281 MAXCHI = 7 x 10^{-16}; CHIMAERA = 4.019 x 10^{-03}; SISCAN = 1.090 x 10^{18} and 3SEQ = 2.969
282 x 10^{-29}. The boundaries of the breakpoints were placed at the end of the *nd2* genes by all
283 methods, extending across the *nd6*, *atp6*, mt*ORF* and ending at the beginning of the *nd4* gene
284 (Supplementary Figure *S3*). A second event, in which the recombinant region was transferred
285 from *Pocillopora* to the *RS_LinB* was hypothesized, in this case the recombinant region was
286 restricted to the *atp6* gene. A third event was detected, by only 3 methods, in *Seriatopora hystrix*
287 *and Seriatopora caliendrum*.
288
289 Family phylogenies focused in *Stylophora* and including the region inherited from the minor
290 parent (*S. pistillata*, Taiwan; 2415 bp) and the major parent (*RS_LinB*; 9555 bp) (Figure 3b)
291 corroborated the phylogenetic patterns outlined for *RS_LinA* and *RS_LinB* in our interspecific
292 phylogenies (Figure 2).

293 **3. DISCUSSION**

294

295 The results from our study show the first evidence of mitochondrial recombination in corals and
296 support the hypothesis that mtDNA introgressive hybridization is the most likely cause of
297 topological mito-mito incongruence in *Stylophora*. Our recombination analyses, using the full
298 mitogenomes of pocilloporid corals (*Madracis, Pocillopora, Seriatopora* and *Stylophora*,
299 including the two Red Sea lineages), provides evidence of mtDNA introgression in this group –
300 particularly in *Stylophora*– strongly suggesting the existence of a hybrid lineage (*RS_LinA*) in
301 the Red Sea, Gulf of Aden and Arabian Gulf.

302

303 The mitogenome of *RS_LinA* contains introgressed genes from two divergent mitochondrial
304 lineages: on mtDNA genes found in the recombinant region (i.e. covering the complete *nd6*, *atp6*
305 and mt*ORF* genes), which have been inherited from a parental species included in a lineage
306 distributed in the Indo-Pacific/Indian Ocean region, while all other mtDNA genes can be traced
307 back to the ancestor of the *RS_LinB*. In the Red Sea, the *RS_LinA* is found in sympatric
308 association with the descendants of its local parental species (*RS_LinB)*, and they harbour
309 different phylogeographic patterns and different *Symbiodinium* composition. In addition, we
310 found that morphospecies placed within the *RS_LinB* agreed with phylogenetic subclades, which
311 accounts for the presence of two divergent allopatric populations divided in northern and
312 southern areas, consistent with environmental and oceanographic discontinuities, a trend that was
313 completely absent in the hybrid *RS_LinA*.

314

315 The colonization of the extreme environments of the Red Sea by the ancestral *RS_LinB* implied
316 the development of adaptations to demanding temperature and salinity conditions. This likely
317 involved selective pressures observed to multiple amino acid changes in mitochondrial proteins,
318 evidenced by the highest substitution rate in the *atp6* and in the mt*ORF* genes of the *RS_LinB*,
319 when compared with other *Stylophora* lineages. For example, the *atp6* gene showed a high
320 number of nucleotide substitutions in the ancestral *RS_LinB*, when compared with the hybrid and
321 the Indo-Pacific/Indian Ocean lineage (i.e. 50 and 45 point mutations respectively), and only few
322 substitutions between the hybrid and its parental Indo-Pacific species (i.e. 8 mutations), which

323 suggest a role of such mtDNA genes in the adaptation to extreme environments. These results
324 have important implications for the conservation of Red Sea species and corals.
325
326 **3.1. Divergent mitochondrial lineages of *Stylophora* are present in the Red Sea**
327
328 Our *atp6*-mt*ORF* phylogenetic analyses highlight the presence of two divergent sympatric
329 *Stylophora* lineages in the Red Sea/Gulf of Aden/Arabian Gulf areas: the *RS_LinA* sharing a
330 common ancestry with an Indo-Pacific/Indian Ocean/Madagascar lineage –placed in Clade 1– and
331 the *RS_LinB* lineage, which form a unique clade on its own –Clade 2– (Figure 2). The existence
332 of these two lineages was reinforced by the family phylogenies of the full *atp6* and *nd6* genes
333 (Figure 3a), which support the hypothesis that the hypervariable mt*ORF* gene, a mitochondrial
334 open reading frame of unknown function, which is unique to the family Pocilloporidae (Flot and
335 Tillier, 2007a), perform as a barcode gene for members of this family (Johnston et al. 2017).
336
337 Noticeable, the *atp6*-mt*ORF* showed topological incongruence with the CR/12S loci (Figures 2b,
338 2c) and the four nuclear genes used in these analyses did not support the existence of *RS_LinA*
339 and *RS_LinB* lineages (Supplementary Figure *S1*). The only nuclear gene that showed a similar
340 phylogenetic pattern of that shown by the CR and 12S genes, was the ITS2, which likely imply
341 that the ITS2, subject to concerted evolution, tells a similar evolutionary history to that of
342 mitochondrial genes.
343
344 Mito-nuclear incongruence such as reported in this study have already been reported in the
345 literature on many metazoans taxa (Willis et al. 2006; Toews, Brelsford 2012; Pavlova et al.
346 2013; Forsman et al. 2017; Salvi et al. 2017) and they are frequently invoked as one of the main
347 signatures of selection (Morales et al. 2015), the result of incomplete lineage sorting (Van Oppen
348 et al. 2001; DeBiasse et al. 2014; Richards and Hobbs 2015) or introgressive hybridization
349 (Diekmann et al. 2001; Gompert et al. 2008; Forsman et al. 2017). The latter is often considered
350 to be rampant in corals, with reticulate evolution having been proposed as one of the main
351 processes that contributed, in great extent, to their successful adaptation after the geographical
352 range expansions induced by several catastrophic events, such as the Cretaceous mass
353 extinctions and the glacial events of the Plio-Pleistocene (Veron 1995). Our finding of

354 incongruity in the phylogenetic patterns among mitochondrial genes versus nuclear genes in
355 *Stylophora*, are therefore consistent with multiples studies in reef building corals.
356
357 In addition, to our knowledge, the degree of incongruence in mtDNA genes found in our
358 analyses has not being identified in others coral genera so far. In *Stylophora*, incongruence
359 between the mt*ORF* and the *CR* topologies was reported by Arrigoni et al. (2016) and Stefani et
360 al. (2011).These authors suggested that the most plausible hypothesis for explaining this finding
361 was the presence of pseudogenes at the mitogenome of this group, but we found no evidence for
362 stop codons or other signs of ORF disruption, rather evidence that this mt*ORF* may code for a
363 functional transmembrane protein (Banguera-Hinestroza et al. unpublished results) as proposed
364 by Flot and Tillier (2007). Therefore, we believe that other hypotheses such as recombination
365 resulting from introgressive hybridization at the mtDNA genome of *Stylophora* are equally
366 probable as the ones discussed in Stefani et al. (2011).
367
368 In species with a uniparental inheritance of mtDNA, genes are linked and are expected to show
369 the same phylogenetic patterns (Ladoukakis and Zouros 2017). However, contrasting topologies
370 in mtDNA genes may arise as the result of mtDNA introgressive hybridization, which is known
371 to have a clear impact in genealogical and phylogenetic reconstructions (White et al. 2008). The
372 presence of divergent mitochondrial genomes in the germline of an organism (heteroplasmy) as
373 the result of paternal leakage (Rokas et al. 2003; Barr et al. 2005; Kuijper et al. 2015) may result
374 in mtDNA recombination (considering that heteroplasmy have remained without modifications
375 in the oocyte cytoplasm long enough for allowing recombination between paternal and maternal
376 mtDNA; White et al., 2008). In the case that the recombinant genome become fixed, viable, and
377 passed to the following generations it would result in viable hybrids carrying a mixed mtDNA
378 genome (Rokas et al. 2003; White et al. 2008; Wilton et al. 2018). Even though, heteroplasmy
379 have not been recorded in reef-building corals, there is an increasing evidence that mtDNA
380 recombination resulting from mtDNA introgressive hybridization is not rare in nature (Rokas et
381 al. 2003; Piganeau et al. 2004; Barr et al. 2005; Levsen et al. 2016).

382 **3.2. mtDNA recombination explains topological incongruence**

383

384 Our recombination analyses hypothesized the *RS_LinA* as a recombinant sequence with high
385 probabilities in all methods (*P*-values ranging between 4.0 x 10^{-03} and 2.96 x 10^{-29}) with the
386 major parent being the sequence from *RS_LinB*, and only the minor parent the sequences from *S.*
387 *pistillata* from Taiwan. For *RS_LinA* the recombinant region –inherited from the minor parent –
388 spans the full *nd6*, *atp6* and mt*ORF* (Supplementary Figure *S3*), which explain that trees
389 constructed with these genes showed a common ancestry between the *RS_LinA* and the Indo-
390 Pacific/Indian ocean/Madagascar lineages, while the same trees show a strong diversification
391 between these two lineages and the *RS_LinB* (Figure 2 and Figure 3). Moreover, the *RS_LinA*,
392 inherited most of its mtDNA genes from the ancestor of *RS_LinB*. Therefore, it is expected that
393 other mtDNA genes display a closest relationship between the *RS_LinA* and the *RS_LinB*, as
394 shown in our phylogenies for the CR and 12S genes and in the mitogenome phylogenies
395 excluding the recombinant region (Figure3b). Consequently, our data strongly supports mtDNA
396 introgressive hybridization followed by recombination as the main cause of mito-mito
397 topological incongruence in *Stylophora*.

398

399 We interpret these results as a strong evidence that *RS_LinA* likely arose from a hybridization
400 event between two ancestral *Stylophora* lineages. The introgression pattern follow that recorded
401 in species of hybrid zones, in which hybrids usually display an unequal mix of two mtDNA
402 genetic backgrounds, with most mitochondrial genes or genetic polymorphism passed from the
403 genetic pool of the local species to the genome of the "invader" species (asymmetric patterns of
404 introgression; Harrison and Larson, 2014).

405

406 **3.3. Interspecific phylogenies and comparative phylogeographic analyses of Red Sea**
407 **lineages**

408

409 As our study focuses at the population level –based on the three most variable genes used here:
410 the *hsp70*, the CR and the *mtORF*– markedly different phylogeographic patterns arises for
411 *RS_LinA* and for *RS_LinB* along the latitudinal and environmental gradient in the Red Sea
412 (Figure 5). These patterns show a strong structure for *RS_LinB*, in which the groups supported by

413 the phylogenetic analyses (Figure 4) have restricted distribution either in the northern Red Sea or
414 in the southern Red Sea, with the break between the two zones found around Yanbu, a trend that
415 was supported by the distribution of the haplotype frequencies along the gradient for each gene
416 (Supplementary Figure *S2*). In contrast, a lack of association with northern and southern
417 environmental provinces was found in members of *RS_LinA*, and rather a clinal variation in
418 haplotype frequencies was found across the gradient (Supplementary Figure *S2*).
419
420 Both lineages were also remarkably different in terms of morphology and *Symbiodinium*
421 association: in the northern Red Sea population of *RS_LinB* (i.e. subclade *LB1*; Figure 4b) most
422 colonies were associated with morphotypes of *Stylophora subseriata* (as described in Veron et al.
423 2018) and *Symbiodinium* type C160; whereas the central-southern population (i.e. subclade LB2;
424 Figure 4b) grouped mostly individuals described in the literature as *Stylophora pistillata* and
425 were associated mainly with *Symbiodinium* type A1, but in contrast to the northern group, no
426 colonies were found carrying C160 or A1-C160 *Symbiodinium* types. Contrary to the trends
427 detected in *RS_LinB*, colonies belonging to the hybrid lineage (*RS_LinA*) showed high
428 phenotypic plasticity and most colonies carried a *Symbiodinium* type A1 in both northern and
429 southern regions (Figure 4).
430
431 The strong differences found in both lineages, in terms of phylogeography, population
432 subdivision, and congruence/incongruence between morphology and phylogenies, reinforces the
433 hypothesis of an early colonization of the Red Sea by members of *RS_LinB* and a recent
434 colonization of *RS_LinA* in agreement with its hybrid origin. This evolutionary scenario could be
435 explained on the light of the multiple processes that have affected the region during the last
436 glacial periods, as well as of the demographic history of reef coral fauna in this region. Several
437 studies targeting the geological dynamic of the Red Sea and the patterns of diversity and
438 endemism of its fauna (Moustafa and Hallock 2008; Rohling et al. 2008; Fine et al. 2013;
439 Moustafa et al. 2014; DiBattista, Howard Choat, et al. 2016; DiBattista, Roberts, et al. 2016)
440 indicate that early coral reefs inhabiting this region (i.e. likely present in the region since the
441 Miocene; Taviani 1998) were able to survive extreme climatic variations in sea levels and
442 periods of hyper salinity (Rohling et al., 2013; Siddall et al., 2003; Righton et al., 1996; Rohling
443 et al., 2013) thanks to the presence of refuge areas in the northern Red Sea (i.e. the Gulf of

444 Aqaba) and in the southern regions (i.e. Southern Red Sea and Gulf of Aden) (Fine et al. 2013;
445 Moustafa et al. 2014; Pellissier et al. 2014). Therefore, isolation in these refuge zones leading to
446 diversification and posterior recolonization may explain the differentiation in allopatry of
447 northern and central-southern populations of *RS_LinB*.
448
449 Furthermore, the phylogeographic patterns, such as the one presented here are also in accordance
450 with several biogeographic studies, showing that oceanographic conditions along the
451 environmental gradient of the Red Sea (Raitsos et al. 2013; Sawall et al. 2015) have originated
452 barriers to genetic flow, influenced strongly the population structure of several species, and
453 shaped patterns of endemism in this region (Nanninga et al. 2014; Saenz-Agudelo et al. 2015;
454 DiBattista, Howard Choat, et al. 2016), despite the fact that they seem to have little impact on
455 reef communities in terms of richness of species and species diversity (Roberts et al. 2016). For
456 example, Nanninga et al. (2013) found a good correlation between the genetic differentiation
457 among anemonefish (*Amphiprion bicinctus*) along the Saudi Arabian coast and the
458 environmental heterogeneity in this basin, with the steadiest genetic break found at
459 approximately 19°N (Southern Red Sea), which coincided with a sharp increase in turbidity in
460 this zone. Results of our study also concur with those of Froukh and Kochzius (2008, 2007) who
461 also found high genetic differentiation that were related to physical differences among fourline
462 wrasse fish (*Larabicus quadrilineatus*) from the northern and southern Red Sea. On a larger
463 scale, research on butterfly and angel fish by Roberts et al. (1992) and studies by DiBattista et al.
464 (2013) have hypothesized that several reef fish species diversified and remained restricted to the
465 Red Sea.
466
467 **3.4. The diversification of *Stylophora* in the Red Sea and Gulf of Aden**
468
469 Our phylogeographic analyses indicate a broad distribution of *RS_LinB* across the Red Sea but
470 limited distribution in the Gulf of Aden (only few 5 out of 37 samples carrying a single mtDNA
471 haplotypes were found in this region, see also Stephani et al. 2017) (Supplementary Figure *S2*),
472 which suggest that the ancestor of *RS_LinB* was likely endemic of these regions, with the border
473 of its distribution in the Gulf of Aden. This lineage likely interbred with a lineage of broader
474 distribution in the Indo-Pacific/Indian-Ocean at the periphery of its range, which is also a

475 confluence between several marine provinces: the Red Sea and Gulf of Aden, the western Indian
476 Ocean, and Indo-Polynesian provinces, at zone that have been shown to hold several hybrid
477 species (DiBattista et al. 2015). Moreover, the phylogenetic position of Arabian Gulf haplotypes,
478 which were placed in the same subclades of the *RS_linA* specimens, implies that the hybrid
479 expanded its range into the Arabian Gulf and into the Red Sea –where it lives in sympatry with
480 the descendants of the parental lineage–
481
482 Our results concur with multiple studies that have identified a large number of hybrid species in
483 the Red Sea (DiBattista, Howard Choat, et al. 2016; Berumen et al. 2017) and seem to fit in the
484 model of hybrid zones and marginal areas (Barton 1979; Hewitt 1988), in which species from a
485 diverse range of taxonomic groups (i.e. plants, yeasts and to a lesser extent animals) living at the
486 edge of their geographic ranges produce viable hybrids carrying recombinant mitogenomes
487 (Rokas et al. 2003; Barr et al. 2005). These hybrids are able to adapt to new climatic conditions,
488 and diverge in sympatric association with their parental species (Rokas et al. 2003; Ballard and
489 Whitlock 2004; Barr et al. 2005; Ujvari et al. 2007; Galtier 2011; Mastrantonio et al. 2016;
490 Leducq et al. 2017; Peris et al. 2017; Fourie et al. 2018).
491
492 In addition, the pattern found in our results in *Stylophora* were similar to those found in hybrid
493 species of marine reef-fishes, found at the intersection of three main biogeographical regions: the
494 Red Sea and Gulf of Aden, the western Indian Ocean and the Indo-Polynesian provinces
495 (DiBattista et al. 2015). These authors identify 14 hybrid species based in molecular markers and
496 morphological characteristics, the gene flow was unidirectional, and the parental species were
497 found at the periphery of their distribution range, where they showed the lowest abundance.
498 Interestingly, as in our work with *Stylophora*, the reported hybrids were found to be the result of
499 intercrosses between endemic species, with restricted distribution range in the Red Sea and
500 Arabian Gulf, with species broadly distributed in the Indo-Pacific, and the major parental species
501 was at the limit of its distribution and almost absent from the Gulf of Aden area.

502 **3.5. Implications for conservation in a climate change scenario**

503

504 Under the current challenges that climatic change poses for coral reef ecosystems, particularly with
505 the rising of oceanic temperatures above the limit threshold of most species (1°C above mean
506 summer maximum) (Pandolfi et al. 2011; Hughes et al. 2018) evolutionary studies with a clear
507 assessment of the demographic history of species and populations are of great relevance,
508 particularly to understand the main mechanisms involved in adaptation and speciation in variable
509 and extreme environments. Our study, coupling recombination analyses, phylogenetic and
510 phylogeographic patterns, suggest that mtDNA genes may play a key role in adaptation to extreme
511 environments in coral species.

512

513 Two genes, the *atp6* gene and the mt*ORF* gene showed high mutation rates and extreme
514 variability in the *RS_LinB* and amino acid and structural changes were recorded mainly at the
515 mt*ORF* protein (Banguera-Hinestroza et al. unpublished data). Two nucleotide changes at
516 positions 104 and 187 in the *atp6* gene revealed multiple paths, resulting in replacement of polar
517 amino acids by non-polar amino acids or vice versa (see results), which we speculate may have
518 led to changes in protein characteristics and function as reported by other authors (see Betts and
519 Russell 2007). Interestingly, the *atp6* protein is not only essential in the oxidative
520 phosphorylation system, responsible for providing the energy required for multiple cellular
521 functions (Saccone et al. 2006) but also is part of a group of genes that are essential in releasing
522 and controlling the proliferation of deleterious oxygen radicals (ROS) in the mitochondria
523 (Kühlbrandt., 2015; Wirth et al., 2016), which are known for causing oxidative damage to
524 symbionts and corals during exposition to high temperatures, with the subsequent bleaching and
525 dead of corals (Downs et al. 2002; Smith et al. 2005). This finding, therefore, support our
526 hypothesis that the multiple mutational changes at the mt*ORF* and *atp6* genes played a key role
527 in the adaptation of *RS_LinB* to the changing environment and habitat conditions of the Red Sea.

528

529 In addition, in *RS_LinB*, the frequencies of the most common haplotypes of the mt*ORF* locus
530 were associated with coldest (north) or hottest (central-south) areas in the Red Sea
531 (Supplementary Figure S2), a tendency that was also followed by the haplotype frequencies of
532 the *hsp70* gene –a chaperone protein involved in heat stress response (Mayer and Bukau 2005;

533 Kvitt et al. 2016)–, suggesting that both proteins may have played a similar role in the adaptation
534 to temperature in *RS_LinB* variants. This premise was supported by the computational
535 characterization of the mt*ORF* protein (Banguera-Hinestroza et al. unpublished) in which
536 searches against approx. 95 million protein domains classified in the CATH data base –using the
537 pDomTHREADER approach (Lobley et al. 2009)–, revealed that domains in the mt*ORF* protein
538 of *RS_LinB*, have the highest matches with annotated domains involved in the structural integrity
539 of a complex or its assembly within or outside a cell (CATH domain code: 1s58A00) and
540 domains that play a role in cell-to-cell, cell-to-matrix interactions, and response to stress
541 (1ux6A01) with high levels of confidence ($0.0001 < P < 0.001$).
542
543 Our findings suggest that selective pressures imposed by the extreme environmental variations in
544 the Red Sea along multiple geological periods, may have had an impact in the mitogenome of
545 this lineage, with consequences in adaptation and speciation, as have been found in other taxa
546 evolving in a broad range of environmental conditions (Hill 2016; Hill 2017; Lamb et al. 2018).
547 Even though the *RS_LinB* hybridized with an Indo-Pacific/Indian Ocean lineage, the resulting
548 hybrid (*RS_LinA*) did not inherited the variation at the *nd6*, *atp6* and mt*ORF* genes, this open the
549 question whether other mitochondrial genes or mtDNA mechanisms may play a role in hybrid
550 speciation and adaptation, or whether the hybrid may be more vulnerable to strong temperature
551 variation (i.e. nowadays the *RS_LinA* is very rare in the Arabian Gulf Area; Banguera-Hinestroza
552 et al. unpublished results).
553
554 Taken together, our data indicate that hybridization in corals and the adaptation of coral hybrids
555 species could be more complex than commonly expected, involving little known mechanisms
556 implicated in mitochondrial metabolism and mitochondrial genome evolution, as have been
557 previoulsy emphasized by Dixon et al., (2015) that demonstrated a strong maternal effect in heat
558 stress tolerance. Assisted hybridization has been proposed as an alternative for conservation of
559 coral reef via genetic rescue (Chan et al. 2018); however, little is known about the molecular
560 mechanisms enhancing hybrid adaptation and speciation under extreme climatic conditions. A
561 clear understanding of these mechanisms coupled with the demographic history of coral
562 populations is therefore needed to pursue effective conservation plans.

563 **4. MATERIAL AND METHODS**

564

565 **4.1. Coral Sampling**

566

567 We sampled a total of 725 colonies of *Stylophora* at 25 locations along the Red Sea coast in 2011
568 and 2012 from the Gulf of Aqaba in the North (Maqna, 28° 31' 34.20 N, 34° 48' 14.30" E) to
569 Farasan Island in the South (16° 31' 38.5" N, 42° 01' 54.09" E). Our sampling design covered the
570 entire environmental gradient (Temperature: ~21 in the north to ~33°C in the south; Salinity: 41
571 PSU in the north to 37 PSU in the south) of the Red Sea and the four oceanographic provinces as
572 defined in Raitsos et al. (2013) (Figure 1 and Supplementary Table *S2*). Colonies were
573 determined to belong to morphotypes of *S. pistillata*, *S. subseriata*, *S. danae*, *S. kuelhmanni* and
574 *S. wellsi* (Figure 1). Identification was carried out with the assistance of Dr. J.E.N Veron
575 (personal communication) and by comparing his photographic records of Red Sea samples with
576 our photographs taken during coral sampling. Small coral nubbins (~1cm) were collected in 3-7
577 m depth from colonies 5 m apart from each other to minimize sampling of clones and were
578 preserved at room temperature in salt-saturated DMSO buffer (Seutin et al. 1991; Gaither et al.
579 2011)

580

581 **4.2. DNA extraction, PCR and sequencing**

582

583 Coral nubbins were placed in approximately 400 µL of lysis buffer (DNeasy Plant Minikit;
584 Qiagen, Hilden, Germany®) with sterile glass beads and beaten for 30 s at full speed in a Qiagen
585 Tissue Lyser II (Qiagen, Hilden, Germany®). After cell lysis, DNA was extracted following the
586 protocol recommended by the manufacturer. Five mitochondrial genes and four nuclear genes
587 were amplified. First we barcoded our samples using the mt*ORF*, which is considered the most
588 variable gene for Pocilloporidae (Flot and Tillier 2007) and a short fragment of the adjacent
589 ATPase subunit 6 gene (*atp6*). After this initial barcoding step, the mitochondrial control region
590 (CR), the cytochrome *c* oxidase subunit I (*cox1*) and the mitochondrial 12S and 16S ribosomal
591 RNA (rRNA) genes were amplified for a subset of samples. A subset was also amplified for
592 several nuclear genes: the heat shock protein (*hsp70*) gene, the internal transcribed spacers (ITS1
593 and ITS2) and the Plasma Membrane Calcium ATPase (*PMCA*) gene. The 16S, 12S and *cox1*

594 were amplified with primers designed in this study. The primers we included and their respective
595 references are listed in the Supplementary Table *S3*.
596
597 After amplification, samples were cleaned using the Exostar 1-step protocol (Ilustra®) and
598 sequenced in both forward and reverse directions; 5-10 specimens of each haplotype were
599 sequenced twice to confirm the accuracy of the sequences. The forward and reverse
600 chromatograms were assembled and edited using Chromas-Pro software version 2.1.5.1
601 (Technelysium, Pty Ltd). Sequences were first aligned using MUSCLE (Edgar 2004) as
602 implemented in MEGA version 7.0.26 (Kumar et al. 2016) and when the resulting alignment
603 contained multiple gaps we used MAFFT's FFT-NS-i (Slow; iterative refinement method) to
604 improve the alignment (Katoh and Standley 2013). All alignments were confirmed and corrected
605 by eye and sequences were trimmed to the same length for further analyses.
606 For 12S and 16S*,* we removed a small region in which a long stretch of homopolymers did not
607 allow high confidence in the alignment. Nuclear genes were phased using the programs PHASE
608 Version 2.1 (Stephens and Donnelly 2003) using the input files obtained in SeqPHASE (Flot
609 2010).
610
611 In the few cases when ITS1, ITS2, or *PMCA* chromatograms showed multiple double peaks (as
612 expected when sequencing a mixture of DNA sequences of unequal length; Flot et al., 2006) the
613 indels from these chromatograms were not considered for downstream analyses and only clean
614 regions with double peaks were included in the phasing process. In addition to our samples from
615 the Red Sea, we amplified and sequenced the 12S and 16S markers of selected specimens from
616 Flot et al. (2011) from several geographic regions (New Caledonia, Japan, Philippines and
617 Madagascar). Moreover, previously published mt*ORF* and CR sequences (Flot et al. 2011;
618 Stefani et al. 2011) as well as *hsp70* sequences (Klueter and Andreakis 2013) from other
619 geographic regions (i.e. Gulf of Aden and Indo-Pacific) as well as from the Red Sea (i.e. mt*ORF*
620 sequences belonging to *S. mamillata*: Arrigoni et al., 2016) were downloaded from the NCBI
621 database and included in our analyses (accession numbers for these samples can be found in the
622 respective references). Finally, we also included *cox1* sequences from Keshavmurthy et al.
623 (2013) that were downloaded from the Dryad Digital Repository: (doi:10.5061/dryad.n2fb2).

624 **4.3. Identification of zooxanthellae (*Symbiodinium*)**

625

626 *Symbiodinium* types were identified by the amplification of the ITS2 rDNA in a set of
627 *Stylophora* samples from the Red Sea collected throughout the same gradient as described above
628 (N=281). We used the DGGE-ITS2 protocol described in LaJeunesse (2002) with the primers
629 and protocols recommended in LaJeunesse et al. (2003). DGGE gels, electrophoresis and PCR
630 conditions are fully described in Arif et al. (2014). Sequences were processed using Chromas-
631 Pro software version 1.7.5 (Technelysium, Pty Ltd) and phylogenetic assignments were built by
632 comparisons with previously published ITS2 sequences in the GeoSymbio data base (Franklin et
633 al. 2012) and the Todd LaJeunesse's database
634 (https://131.204.120.103/srsantos/symbiodinium/sd2_ged/database/views.php).

635

636 **4.4. Sequence variation, phylogenetic and phylogeographic analyses**

637

638 Number of haplotypes (h), polymorphic sites per gene, and shared haplotypes within and among
639 Red Sea regions (Maqna, Al-Wajh, Yanbu, Kaust, Jeddah, Doga, Farasan and Gulf of Aden;
640 Figure 1) as well as for other geographic locations (see above), were calculated using Arlequin
641 version 3.5 (Excoffier and Lischer 2010) and DNAsp version 5.1 (Librado and Rozas 2009).
642 Phylogenetic analyses were performed using *Stylophora* specimens from seven geographic
643 regions (Caledonia, Japan, Philippines, Madagascar, Gulf of Aden, Arabian Gulf and Red Sea).
644 When several sequences shared the same haplotype, a single representative was included in the
645 data set for phylogenetic analyses.

646

647 To account for the phylogenetic signal in indels (insertion-deletion polymorphism) gaps were
648 treated as missing data and coded as additional presence/absence (0-1) characters with the
649 program Fastgap v1.2. (Borchsenius 2009) resulting in a data set with two data partitions:
650 nucleotides and standard characters (0-1). This approach was used to infer Bayesian trees with a
651 mixed model, which allows the combination of different data partitions with parameters unlinked
652 across partitions (Huelsenbeck and Ronquist 2001). The best evolutionary models for each gene
653 and data partition were selected by calculating their BIC (Bayesian Information Criterion) scores
654 as recommended in MEGA v.7 (Kumar et al. 2016). The non-uniformity of evolutionary rates

655 among sites was modelled using a discrete Gamma distribution (+G) with 5 rate categories and
656 by assuming a portion of the sites to be invariant (+I). The gamma shape parameter, proportion
657 of invariant sites, transition/transversion ratio, nucleotide frequencies and rates of substitutions
658 were also estimated from the data.
659
660 Bayesian trees were built in MrBayes (Huelsenbeck and Ronquist 2001) at the CIPRES Science
661 Gateway v 3.1 (Miller et al. 2010). For each data set we performed 4 independent runs (nruns=4)
662 with 1 cold and 3 heated chains (nchains=4). The total number of generations (ngen) was set at
663 10,000,000; sampling was performed every 1000 generations (Diagnfreq=1000); and the burn-in
664 fraction was set to 25% (burninfrac=0.25). Convergence was assessed using the program Tracer
665 v 1.7 (Rambaut and Drummond 2009). Maximum Likelihood (ML) and Neighbor Joining (NJ
666 trees) were built in MEGA v.7 (Kumar et al. 2016), with 1000 bootstrap replicates. We used the
667 nearest neighbor interchange algorithm (NNI) with an initial tree automatically generated
668 (option: NJ/BioNJ) and the branch-swap filter set to strong, including all sites in the alignment.
669
670 NJ trees were constructed using the Maximum Composite Likelihood method, with the pairwise
671 deletion option activated. Trees were constructed for all markers, except 16S and *cox1* that
672 showed little or no variability in *Stylophora* spp. (see results). mt*ORF* and CR phylogenies
673 (using our complete data set) were built only using the alignable regions among all samples and
674 the outgroups (*Pocillopora* and *Seriatopora*), and alternatively, excluding the outgroups to allow
675 the analyses of longer fragments (in these cases, the root of the trees was placed in agreement
676 with that inferred by the phylogeny using shorter fragments and by the loci in which the full
677 outgroup sequences were included).
678
679 Relationships among haplotypes were explored for the three most variable markers (mt*ORF*, CR
680 and *hsp70*) using the program HaplowebMaker (https://eeg-ebe.github.io/HaplowebMaker/;
681 Spöri and Flot, in prep.) applying the median-joining algorithm. Haplotypes belonging to
682 specimens from the Pacific regions and Madagascar were included, when possible, to identify
683 patterns of colonization. The frequency of each haplotype along the environmental gradient of
684 the Red Sea (i.e. each locality/population) was calculated using Arlequin v. 3.5 (Excoffier and
685 Lischer 2010).

686 **4.5. Mitogenomes assembly and annotation**

687

688 The complete mitogenomes of the two Red Sea lineages identify in our individual phylogenies
689 analyses (see results) –called *RS_LinA* and *RS_LinB*– were obtained using two different
690 approaches. First, paired-end Illumina reads from the draft genome of *Stylophora pistillata*
691 (Voolstra et al. 2017) –identified as *RS_LinA*– were downloaded from the NCBI Short Read
692 Archive (https://www.ncbi.nlm.nih.gov/sra/SRX999949) using fastq-dump (fastq-dump --
693 origfmt --split-3 SRR1980974). Second, 1.7 Gb paired-end reads for the *RS_LinB* were obtained
694 from Red Sea samples preserved in CHAOS buffer (Flot 2007) and extracted using the DNA
695 NucleoSpin kit (Macherey-Nagel) following the protocol recommended by the company.
696 Sequencing was performed in an Illumina NovaSeq 6000 at the BRIGHTcore facilities (Brussels
697 Interuniversity Genomics High Throughput core)

698

699 The mitogenome of both lineages were assembled de novo from the raw Illumina reads using
700 NOVOPlasty v2.7.1 (Dierckxsens et al. 2016) with the *cox1* gene as a seed. For the assembly of
701 the *RS_LinB* mitogenome, both *cox1* and the complete mitogenome of the *RS_LinA* were used as
702 seeds. Runs were performed without and with reference, using the mitogenome of *Stylophora*
703 *pistillata* (NC_011162.1) for comparative purposes. The accuracy of the assembly was confirmed
704 by mapping the reads back to the assembled genomes using Bowtie2. In addition, the identity of
705 each lineage was corroborated by aligning the resulting genomes with sequences from six of the
706 markers used for our interspecific phylogenies (mt*ORF*, CR, *atp6*, 12S, 16S and *cox1*). Genes
707 were annotated using MITOS (Bernt et al. 2013; Al Arab et al. 2017). Alignment for each
708 annotated gene was performed with MUSCLE (Edgar 2004) and genes identities were confirmed
709 using BLAST searches. When there was incongruence, particularly at the 5' and 3' ends of the
710 genes, annotations were manually corrected using as reference standard (RefSeq) the
711 mitogenome of *Stylophora pistillata* from the NCBI data base (NC_011162.1). Finally, genes
712 were concatenated using Fastgap v1.2. (Borchsenius 2009) and aligned with mitogenomes from
713 other members of the family Pocilloporidae using MAFFT (Katoh and Standley 2013). The
714 mitogenomes included were: *Seriatopora hystrix* (EF633600.2), *Seriatopora caliendrum*
715 (EF633601.2), *Pocillopora damicornis* (EF526302.1; EU400213.1), *Pocillopora eydouxi*

716 (EF526303.1), *Stylophora pistillata* (of Indo-Pacific origin; NC_011162.1) and *Madracis*
717 *mirabilis* (EU400212.1).

718 **4.6. Analyses of recombination and mitogenome phylogenies**

719

720 Recombination was tested using the alignments of the full mitogenomes from members of the
721 family Pocilloporidae*,* including the two divergent *Stylophora* lineages from the present study –
722 see results–; the genus *Polyciathus* was also included as an external sequence. Seven heuristic
723 recombination detection methods implemented in the RDP4 package (Martin et al. 2015) were
724 used: RDP (Martin et al. 2010), BOOTSCAN (Martin et al. 2005), GENECONV (Padidam et al.
725 1999), MAXCHI (Maximum Chi Square method; Smith 1992); CHIMAERA (Posada and
726 Crandall 2001), SISCAN (Sister Scanning method; Gibbs et al. 2000), and 3SEQ (Boni et al.
727 2006).

728

729 The default settings were used for most methods, except for window sizes, step sizes and tree
730 building methods. Window size was selected to include at least 10 variable nucleotide positions
731 within every window examined. In RPD, SISCAN, and BOOTSCAN methods windows size
732 were set at 100; in CHIMAERA and MAXCHI at 200. Alternatively, the MAXCHI and
733 CHIMAERA methods were set to run with variable windows sizes, to allow the program to
734 adjust the window size depending on degrees of parental sequence divergence as recommended
735 by the author. Only recombination events detected with $P<0.05$, after Bonferroni correction were
736 recorded.

737

738 The boundaries of the breakpoints were double checked by comparing the agreement of the
739 boundaries between methods. The major parent and the minor parent hypothesized by the
740 program, were contrasted against evidence from our phylogenetic and phylogeographic analyses.
741 Furthermore, given that the parental ascription of the recombinant sequence may be difficult
742 among closely related sequences, we refined the hypothesis by comparing the hypothesized
743 distribution range of the major *Stylophora* clades (Keshavmurthy et al. 2013) and the supporting
744 data from previous studies in hybrids species in the region and outside the Red Sea (DiBattista et
745 al. 2015). It is important to note that the identified major and minor parents are not the "real"

746 parental sequences, but sequences that are closely related to likely ancestral sequences, also that
747 the recombinant region is related to the "minor" parent and the "non-recombinant" region related
748 to the "major" parent (Martin et al. 2015).
749
750 Phylogenetic relationships among mitogenomes were inferred using maximum likelihood trees in
751 PhylML (Guindon et al. 2010) available at the http://www.phylogeny.fr/index.cgi (Dereeper et
752 al. 2008; Dereeper et al. 2010). Branch support was evaluated using an Approximate Likelihood
753 Ratio test (aLRT) (Anisimova and Gascuel 2006). Trees were built for: (a) the full alignments,
754 including and excluding the recombinant region and (b) genes within the recombinant region.
755 The best model was selected as indicated in MEGA v7 (Kumar et al. 2016) as the GTR+G+I
756 (General Time Reversible mode, non-uniformity of evolutionary rates among sites modeled
757 using a discrete Gamma distribution with 5 rate categories and a fraction invariable sites).
758
759 Because ambiguously aligned regions or highly divergent sequences can mislead recombination
760 signals, we ran the analyses including and excluding the *mtORF* and the *atp8* gene, and also
761 excluding ambiguously aligned regions within the mt*ORF*. Finally, to discard the influence of
762 highly divergent sequences, we repeated the recombination analyses excluding the mitogenomes
763 of *Madracis* and *Polyciathus*. After analyses, polymorphic sites in hypervariable genes within
764 the recombinant region for each *Stylophora* lineage were calculated using DNAsp version 5.1
765 (Librado and Rozas 2009).
766
767 **Funding statement**
768
769 This work was supported by King Abdullah University of Science and Technology (KAUST),
770 Saudi Arabia (sample analysis), by King Abdulaziz University (KAU) as part of the Jeddah
771 Transect project (sample collection), and by a postdoctoral research fellowship from the
772 Université libre de Bruxelles, Belgium.
773
774 **Acknowledgments**: The authors want to thank Dr. Veron for assistance with voucher
775 identification, Dr. Saenz Agudelo for sample collections and recommendations, Dr. Bouwmeester
776 for sample collection, Vanessa Robitzch for helping with the DNA extractions, Catalina Ramirez

for her support in bioinformatics pipelines and Sebastien Santini - CNRS/AMU IGS UMR7256, for its effort in maintaining the excellence of the Phylogeny.fr site. Thanks also to Sandra Cervantes Arango, Dario Ojeda Alayon for useful discussions and advices during the preparation of this manuscript. We thanks to King Abdulaziz University (KAU) and the Bioscience Core Lab at KAUST for sharing their facilities.

Supplementary Table *S1*. Sampling sites in the Red Sea and geographic coordinates

Locations	***Reef***	***[a]Ns***	***[b]Nt***	***[c]Nseq***	***Coordinates***		***Depth***
MAQNA	R1	30			28° 31' 34.20"	34° 48' 14.30"	3-5
	R2	37	67	67	28° 25' 36.48"	34° 45' 06.17"	3-7m
AL-WAJH	R1	59			26° 11' 15.05"	36° 20' 57.21"	1-3m
	R2	2			26° 09' 59.80"	36° 23' 32.20"	3m
	R3	24			26° 14' 28.3"	36° 26' 25.3"	5-10m
	R4	28	113	113	26° 11' 06.2"	36° 22' 58.9"	3-7m
YANBU	R1	28			23° 56' 50.70"	38° 10' 31.80"	6-10
	R2	16			23° 54' 58.92"	38° 09' 00.63"	6-10
	R3	28			23° 57' 19.20"	38° 12' 16.00"	3-5m
	R4	29			23° 54' 41.4"	38° 09' 08.4"	3-7m
	R5	17	118	118	----------	----------	2-10m
KAUST	R1	42			22° 19' 09"	38° 51' 16"	1-7m
	R2	46			22° 04' 02"	38° 46' 09"	2-8m
	R3	47	135	135	22° 30' 48"	38° 55' 17"	2-10m
JEDDAH	R1	30			21° 45' 11.40"	38° 57' 45.09"	1-3m
	R2	20			21° 46' 06.3"	38° 57' 47.07"	2-5m
	R3	20	70	64	21° 41' 23.26"	39° 00' 49.05"	N/A
DOGA	R1	29			19° 38' 06.40"	40° 34' 31.30"	3-5m
	R2	29			19° 36' 50.50"	40° 38' 17.50"	3-5m
	R3	30	88	88	19° 39' 56.49"	40° 37' 21.59"	3-5m
FARASAN	R1	30			16° 34' 45.50"	42° 08' 57.50"	4-5m
	R2	30			16° 34' 44.38"	42° 14' 11.47"	3-5m
	R3	20			16° 31' 30.65"	42° 01' 57.11"	3-4m
	R4	30			16° 31' 38.5"	42° 01' 54.09"	3-6m
	R5	24	134	131	----------	----------	1-5m
Total			**725**	**716**			

[a] = Total number of samples per reef; [b] = Total number of samples per region; [c] = Total number of sequences obtained for the mt*ORF* gene

Supplementary Table *S2*. Polymorphic sites per gene

	ALL REGIONS					RED SEA				
Locus	**Nseq**	**size (bp)**	**Polymorphic sites**	**Indels**	**Parsimony informative sites**	**Nseq**	**size (bp)**	**Polymorphic sites**	**Indels**	**Parsimony informative sites**
nDNA genes										
ITS1	75	416	69	94	54	44	416	33	31	16
ITS2	56	329	90	22	68	42	329	44	3	26
PMCA	86	956	107	65	100	50	956	26	11	18
hsp70	738	732	119	2	70	646	732	91	2	33
mtDNA genes										
atp6-mtORF (all samples)	827	545	108	99	107	714	545	102	63	102
atp6-mtORF (Clade 1)	461	884	48	291	40	353	884	10	255	9
Atp6-mtORF (Clade 2)	366	943	22	207	21	361	943	22	207	21
CR	401	757	68	146	65	325	757	3	146	3
12s	72	1381	33	0	33	50	1381	6	0	5
16s	61	1393	7	0	7	43	1393	1	0	1
COI	147	848	19	0	12	110	848	0	0	0

Supplementary Table *S3.* Primers and their respective references

Nuclear loci	Reference	Primer name	sequence (5'-3')
ITS1	Flot et al. 2011	F18S1	CGATYGAAYGGTTTAGTGAGGC
ITS1	Flot et al. 2011	ITSc1-3	CATTTGCGTTCAAAGATTCG
ITS2	LaJeunesse 2007	ITSrev_LaJ	GGG ATC CAT ATG CTT AAG TTC AGCGGG T
ITS2	LaJeunesse 2007	Scler5.8SbF_LaJ	GAA GAA CGC AGCCAA CTG CGA
hsp70	Schmidt-Roach et al. 2013	HSP70A-F	CCTGGTTCAATCCGACAGA
hsp70	Schmidt-Roach et al. 2014	HSP70A-R	TGTTCAGCTGTTTTCCTTCG
PMCA	Zoccola et al. 2004	PMCA_R1	AGGTGGCAGGATGCCACATTT
PMCA	Zoccola et al. 2005	PMCA_R2	GGGCCACACTTCATCAAACTT
PMCA	Zoccola et al. 2006	PMCA_R3	ATTGCGCCCCCACATAACAGC
PMCA	Zoccola et al. 2007	PMCA_F1	TTGCTTTCAAATGTGGCATCC
PMCA	Zoccola et al. 2008	PMCA_F2	GTTAAAGCTGTTATGTGGGGG
Mitochondrial loci			
ORF	Flot et al. 2011	FATP6.1	TTTGGGSATTCGTTTAGCAG
ORF	Flot et al. 2011	RORF	SCCAATATGTTAAACASCATGTCA
CR	Flot et al. 2011	FNAD5.2deg	GCCYAGRGGTGTTGTTCAAT
CR	Flot et al. 2011	RCOI3deg	CGCAGAAAGCTCBARTCGTA
12S	This study	Ser_12s_F	TGTCTTTGGCGAACATGGGT
12S	This study	Ser_12s_R	AGGCCAAACGACTCCAAGTT
12S	This study	Ser_12s_IntF1	GGGGGATTGTGCCTTTTCCT
12S	This study	Ser_12s_IntF2	GCTTGAGTAGTACGGTCGCA
16S	This study	Sty_16s_F	GTGCCGGGTTTATATACCGGT
16S	This study	Sty_16s_R	AAAGGCCAACCCCTTCTCAC
16S	This study	Sty_16s_IntR_2	AATCCCCGCTCCTCTTTCTC
16S	This study	Sty_16s_IntR_3	GGCTGGTTCCAAGCCTACAT
COI	This study	Sty_COXI_F	TTTTTGGTGGAGGTGCTGGT
COI	This study	Sty_COXI_R	TGACCACCACAAGCACAACT

Figure legends

Figure 1. Sampling localities and *Stylophora* morphotypes. **a)**. General map showing the sampling sites. Red stars indicate sequences or samples obtained from published work and yellow stars specify samples collected for this study. **b)**. Map indicating sampling sites along the environmental gradient of the Red Sea. The numbers in parenthesis show the reefs visited at each location. The map was modified from the original downloaded from https://www7320.nrlssc.navy.mil/global_ncom/glb8_3b/html/Links/red/temp_glb8_3b_2012060700_0000m.gif. **c)**. *Stylophora* morphotypes included in this study.

Figure 2. Mitochondrial phylogenies of the genus *Stylophora*. **a)**. Bayesian tree of the *ATP6*-mt*ORF* locus. **b)**. Bayesian tree for the CR gene. **c)**. Maximum Likelihood (ML) tree for the 12S gene. Node support are given in Bayesian Probabilities (BPP) for the mt*ORF*, BPP/ML for the mtCR and ML/NJ for the 12S. Colors are as follow: Red: Haplotypes from Arabian Gulf, Red Sea and Gulf of Aden placed in Clade 1 (*RS_LinA*). Yellow: haplotypes from Madagascar. Green: haplotypes from Indo-Pacific (Philippines, Okinawa, New Caledonia) and Blue: Red Sea and Gulf of Aden haplotypes placed in Clade 2 (*RS_LinB).* Haplotypes names are given in agreement to the region where the haplotype was found in higher frequency (MAQ=MAQNA, WAJ=ALWAJH, YAN=YANBU, KAUST = KAUST, JEDDAH=JED, DOG = DOGA, FARASAN = FAR)

Figure 3. Mitochondrial phylogenies of the family Pocilloporidae and phylogenies derived from the recombination analyses. **a)**. Position of the *RS_LinA* and *RS_LinB* in a family phylogeny of the full *atp6* (above) and *nd6* genes (below). **b)**. ML phylogenies from the recombination hypotheses: phylogeny derived from the recombinant region –minor parent–, including the *nd6*, *atp6*, and *mtORF* genes; 2415bp (above) and phylogeny from mtDNA genes outside the recombinant region –from the major parent –, 9555bp (below).

Figure 4. Extended *atp6*-mtORF phylogenies for **a)**. Clade 1. Highlighting the *RS_LinA* lineage (magenta) and the different subclades within this group. **b)**. Clade 2. Exclusively composed by Red Sea/Gulf of Aden specimens (*RS_LinB*). The two subclades within *RS_LinB* correspond with northern (colder) and central-southern (hotter) regions. The relationship among haplotypes, morphotypes, and *Symbiodinium* types are shown for each lineage.

Figure 5. Network trees showing the relations among haplotypes for the three more variable genes. **a)**. *atp6*-mt*ORF*. **b)**. Control Region (CR) **c)**. *hsp70*. Vertical lines indicate the number of mutations.

Supplementary Figure *S1*. Nuclear phylogenies of the genus *Stylophora*. Bayesian trees for nuclear genes. **a)**. ITS1 b. **b)** ITS2 **c)**. *hsp70* **d)**. *PMCA*. Colors and haplotypes names are in agreement with those in the mt*ORF* phylogenies (see legend in Figure 2). In the *hsp70* phylogeny numbers in parenthesis correspond to the number of specimens found per haplotype in each lineage: *RS_LinA*, *RS_linB.*

Supplementary Figure *S2*. Distribution of haplotype frequencies for the most common haplotypes of the most variable genes across the environmental gradient of the Red Sea. Frequencies are indicated as per mtDNA lineage. The axis x represents relative frequencies. ***S2*a.** *atp6*-mt*ORF* locus ***S2*b**. CR *gene*,

46 and ***S2c.*** *hsp70* gene, including all haplotypes (above) and dividing haplotypes per mtDNA lineage
47 (below).
48
49 **Supplementary Figure *S3*.** Identification of recombinant sequences and estimation of break points by
50 different methods **a)**. CHIMAERA **b)**. MAXCHI, and **c)**. BURT

REFERENCES

Acker J, Leptoukh G, Shen S, Zhu T, Kempler S. 2008. Remotely-sensed chlorophylla observations of the northern Red Sea indicate seasonal variability and influence of coastal reefs. J. Mar. Syst. 69:191–204.

Al Arab M, Höner zu Siederdissen C, Tout K, Sahyoun AH, Stadler PF, Bernt M. 2017. Accurate annotation of protein-coding genes in mitochondrial genomes. Mol. Phylogenet. Evol. 106:209–216.

Anisimova M, Gascuel O. 2006. Approximate Likelihood-Ratio Test for Branches: A Fast, Accurate, and Powerful Alternative. Sullivan J, editor. Syst. Biol. 55:539–552.

Arrigoni R, Benzoni F, Terraneo TI, Caragnano A, Berumen ML. 2016. Recent origin and semi-permeable species boundaries in the scleractinian coral genus *Stylophora* from the Red Sea. Sci. Rep. 6:34612.

Ballard JWO, Rand DM. 2005. The Population Biology of Mitochondrial DNA and its phylogenetic implications. Annu. Rev. Ecol. Evol. Syst. 36:621–642.

Ballard JWO, Whitlock MC. 2004. The incomplete natural history of mitochondria. Mol. Ecol. 13:729–744.

Barr CM, Neiman M, Taylor DR. 2005. Inheritance and recombination of mitochondrial genomes in plants, fungi and animals. New Phytol. 168:39–50.

Barton NH. 1979. The dynamics of hybrid zones. Heredity. 43:341–359.

Bernt M, Donath A, Jühling F, Externbrink F, Florentz C, Fritzsch G, Pütz J, Middendorf M, Stadler PF. 2013. MITOS: Improved de novo metazoan mitochondrial genome annotation. Mol. Phylogenet. Evol. 69:313–319.

Berumen ML, DiBattista JD, Rocha LA. 2017. Introduction to virtual issue on Red Sea and Western Indian Ocean biogeography. J. Biogeogr. 44:1923–1926.

Boni MF, Posada D, Feldman MW. 2006. An exact nonparametric method for inferring mosaic structure in sequence triplets. Genetics 176:1035–1047.

Brennan AC, Woodward G, Seehausen O, Muñoz-Fuentes V, Moritz C, Guelmami A, Abbott RJ, Edelaar P. 2014. Hybridization due to changing species distributions: Adding problems or solutions to conservation of biodiversity during global change? Evol. Ecol. Res. 16:475–491.

Chan WY, Peplow LM, Menéndez P, Hoffmann AA, van Oppen MJH. 2018. Interspecific hybridization may provide novel opportunities for coral reef restoration. Front. Mar. Sci. 5:1–15.

Chen C, Chiou C-Y, Dai C-F, Chen CA. 2008. Unique mitogenomic features in the scleractinian family pocilloporidae (scleractinia: astrocoeniina). Mar. Biotechnol. 10:538–553.

Chinnery PF, Hudson G. 2013. Mitochondrial genetics. Br. Med. Bull. 106:135–159.

Combosch DJ, Vollmer S V. 2015. Trans-Pacific RAD-Seq population genomics confirms introgressive hybridization in Eastern Pacific *Pocillopora* corals. Mol. Phylogenet. Evol. 88:154–162.

DeBiasse MB, Nelson BJ, Hellberg ME. 2014. Evaluating summary statistics used to test for incomplete lineage sorting: mito-nuclear discordance in the reef sponge *Callyspongia vaginalis*. Mol. Ecol. 23:225–238.

Dereeper A, Audic S, Claverie J-MM, Blanc G. 2010. BLAST-EXPLORER helps you building datasets for phylogenetic analysis. BMC Evol. Biol. 10:8.

Dereeper A, Guignon V, Blanc G, Audic S, Buffet S, Chevenet F, Dufayard J, Guindon S, Lefort V, Lescot M, et al. 2008. Phylogeny.fr: robust phylogenetic analysis for the non-specialist. Nucleic Acids Res. 36:W465–W469.

DiBattista JD, Berumen ML, Gaither MR, Rocha LA, Eble JA, Choat JH, Craig MT, Skillings DJ,

Bowen BW. 2013. After continents divide: comparative phylogeography of reef fishes from the Red Sea and Indian Ocean. J. Biogeogr. 40:1170–1181.

DiBattista JD, Howard Choat J, Gaither MR, Hobbs J-PA, Lozano-Cortés DF, Myers RF, Paulay G, Rocha LA, Toonen RJ, Westneat MW, et al. 2016. On the origin of endemic species in the Red Sea. J. Biogeogr. 43:13–30.

DiBattista JD, Roberts MB, Bouwmeester J, Bowen BW, Coker DJ, Lozano-Cortés DF, Howard Choat J, Gaither MR, Hobbs J-PA, Khalil MT, et al. 2016. A review of contemporary patterns of endemism for shallow water reef fauna in the Red Sea. J. Biogeogr. 43:423–439.

DiBattista JD, Rocha LA, Hobbs J-PA, He S, Priest MA, Sinclair-Taylor TH, Bowen BW, Berumen ML. 2015. When biogeographical provinces collide: hybridization of reef fishes at the crossroads of marine biogeographical provinces in the Arabian Sea. J. Biogeogr. 42:1601–1614.

Diekmann OE, Bak RP, Stam W, Olsen J. 2001. Molecular genetic evidence for probable reticulate speciation in the coral genus *Madracis* from a Caribbean fringing reef slope. Mar. Biol. 139:221–233.

Dierckxsens N, Mardulyn P, Smits G. 2016. NOVOPlasty: de novo assembly of organelle genomes from whole genome data. Nucleic Acids Res. 45:gkw955.

Dixon GB, Davies SW, Aglyamova G V., Meyer E, Bay LK, Matz M V. 2015. Genomic determinants of coral heat tolerance across latitudes. Science. 348:1460–1462.

Dokianakis E, Ladoukakis ED. 2014. Different degree of paternal mtDNA leakage between male and female progeny in interspecific *Drosophila* crosses. Ecol. Evol. 4:2633–2641.

Downs CA, Fauth JE, Halas JC, Dustan P, Bemiss J, Woodley CM. 2002. Oxidative stress and seasonal coral bleaching. Free Radic. Biol. Med. 33:533–543.

Edgar RC. 2004. MUSCLE: multiple sequence alignment with high accuracy and high throughput. Nucleic Acids Res. 32:1792–1797.

Ehrenberg CG. 1834. Die Corallenthiere des Rothen Meeres physiologisch untersucht un systematisch verzeichnet. gedruckt in der Druckerei der K. Akademie der Wissenschafte, Berlin (156)

Esper EJC. 1797. Fortsetzungen der Pflanzenthiere in Abbildungen nach der Natur mit Farben erleuchtet nebst Beschreibungen. Erster Theil. Raspische Buchhandlung, Nürnberg.

Excoffier L, Lischer HEL. 2010. Arlequin suite ver 3.5: A new series of programs to perform population genetics analyses under Linux and Windows. Mol. Ecol. Resour. 10:564–567.

Fine M, Gildor H, Genin A. 2013. A coral reef refuge in the Red Sea. Glob. Chang. Biol. 19:3640–3647.

Flot JF. 2010. seqphase: a web tool for interconverting phase input/output files and fasta sequence alignments. Mol. Ecol. Resour. 10:162–166.

Flot JF, Blanchot J, Charpy L, Cruaud C, Licuanan WY, Nakano Y, Payri C, Tillier S. 2011. Incongruence between morphotypes and genetically delimited species in the coral genus *Stylophora*: phenotypic plasticity, morphological convergence, morphological stasis or interspecific hybridization? BMC Ecol. 11:22.

Flot JF, Tillier S. 2007. The mitochondrial genome of *Pocillopora* (Cnidaria: Scleractinia) contains two variable regions: The putative D-loop and a novel ORF of unknown function. Gene. 401:80–87.

Flot JF, 2007. Towards a molecular taxonomy of corals of the genus *Pocillopora*. Ph.D. thesis (Muséum national d'Histoire naturelle, Paris).

Flot JF, Tillier A, Samadi S, Tillier S. 2006. Phase determination from direct sequencing of length-variable DNA regions. Mol. Ecol. Notes. 6:627–630.

Forsman ZH, Knapp ISS, Tisthammer K, Eaton DAR, Belcaid M, Toonen RJ. 2017. Coral hybridization or phenotypic variation? Genomic data reveal gene flow between *Porites lobata* and *P. Compressa*. Mol. Phylogenet. Evol. 111:132–148.

Fourie G, Van der Merwe NA, Wingfield BD, Bogale M, Wingfield MJ, Steenkamp ET. 2018. Mitochondrial introgression and interspecies recombination in the *Fusarium fujikuroi* species complex. IMA Fungus 9:37–63.

Froukh T, Kochzius M. 2007. Genetic population structure of the endemic fourline wrasse (*Larabicus quadrilineatus*) suggests limited larval dispersal distances in the Red Sea. Mol. Ecol. 16:1359–1367.

Froukh T, Kochzius M. 2008. Species boundaries and evolutionary lineages in the blue green damselfishes *Chromis viridis* and *Chromis atripectoralis* (Pomacentridae). J. Fish Biol. 72:451–457.

Gaither MR, Szabó Z, Crepeau MW, Bird CE, Toonen RJ. 2011. Preservation of corals in salt-saturated DMSO buffer is superior to ethanol for PCR experiments. Coral Reefs 30:329–333.

Galtier N. 2011. The intriguing evolutionary dynamics of plant mitochondrial DNA. BMC Biol. 9:61.

Gibbs MJ, Armstrong JS, Gibbs AJ. 2000. Sister-Scanning: a Monte Carlo procedure for assessing signals in recombinant sequences. Bioinformatics. 16:573–582.

Gompert Z, Forister ML, Fordyce JA, Nice CC. 2008. Widespread mito-nuclear discordance with evidence for introgressive hybridization and selective sweeps in Lycaeides. Mol. Ecol. 17:5231–5244.

Guindon S, Dufayard J-F, Lefort V, Anisimova M, Hordijk W, Gascuel O. 2010. New Algorithms and Methods to Estimate Maximum-Likelihood Phylogenies: Assessing the Performance of PhyML 3.0. Syst. Biol. 59:307–321.

Harrison RG, Larson EL. 2014. Hybridization, Introgression, and the Nature of Species Boundaries. J. Hered. 105:795–809.

Hellberg ME, Prada C, Tan MH, Forsman ZH, Baums IB. 2016. Getting a grip at the edge: recolonization and introgression in eastern Pacific *Porites* corals. J. Biogeogr. 43:2147–2159.

Hewitt GM. 1988. Hybrid zones-natural laboratories for evolutionary studies. Trends Ecol. Evol. 3:158–167.

Hill GE. 2016. Mitonuclear coevolution as the genesis of speciation and the mitochondrial DNA barcode gap. Ecol. Evol. 6:5831–5842.

Hill GE. 2017. The mitonuclear compatibility species concept. Auk. 134:393–409.

Huelsenbeck JP, Ronquist F. 2001. MRBAYES: Bayesian inference of phylogenetic trees. Bioinformatics. 17:754–755.

Hughes TP, Kerry JT, Baird AH, Connolly SR, Dietzel A, Eakin CM, Heron SF, Hoey AS, Hoogenboom MO, Liu G, et al. 2018. Global warming transforms coral reef assemblages. Nature 556:492–496.

Johannesson K, Carl A. 2006. Life on the margin: genetic isolation and diversity loss in a peripheral marine ecosystem, the Baltic Sea. Mol. Ecol. 15:2013–2029.

Johnston EC, Forsman ZH, Flot J-F, Schmidt-Roach S, Pinzón JH, Knapp ISS, Toonen RJ. 2017. A genomic glance through the fog of plasticity and diversification in *Pocillopora*. Sci. Rep. 7:5991.

Katoh K, Standley DM. 2013. MAFFT Multiple Sequence Alignment Software Version 7: Improvements in Performance and Usability. Mol. Biol. Evol. 30:772–780.

Keshavmurthy S, Yang S-Y, Alamaru A, Chuang Y-Y, Pichon M, Obura D, Fontana S, De Palmas S, Stefani F, Benzoni F, et al. 2013. DNA barcoding reveals the coral "laboratory-rat", *Stylophora pistillata* encompasses multiple identities. Sci. Rep. 3:1520.

Kivisild T. 2015. Maternal ancestry and population history from whole mitochondrial genomes. Investig. Genet. 6:3.

187 Klueter A, Andreakis N. 2013. Assessing genetic diversity in the scleractinian coral *Stylophora pistillata*
188 (Esper 1797) from the Central Great Barrier Reef and the Coral Sea. Syst. Biodivers. 11:67–76.
189 Kühlbrandt W. 2015. Structure and function of mitochondrial membrane protein complexes. BMC Biol.
190 13:89.
191 Kuijper B, Lane N, Pomiankowski A. 2015. Can paternal leakage maintain sexually antagonistic
192 polymorphism in the cytoplasm? J. Evol. Biol. 28:468–480.
193 Kumar S, Stecher G, Tamura K. 2016. MEGA7: Molecular Evolutionary Genetics Analysis Version 7.0
194 for Bigger Datasets. Mol. Biol. Evol. 33:1870–1874.
195 Kvitt H, Rosenfeld H, Tchernov D. 2016. The regulation of thermal stress induced apoptosis in corals
196 reveals high similarities in gene expression and function to higher animals. Sci. Rep. 6:30359.
197 Ladoukakis ED, Zouros E. 2017. Evolution and inheritance of animal mitochondrial DNA: Rules and
198 exceptions. J. Biol. Res. 24:1–7.
199 Lamb AM, Gan HM, Greening C, Joseph L, Lee YP, Morán-Ordóñez A, Sunnucks P, Pavlova A. 2018.
200 Climate-driven mitochondrial selection: A test in Australian songbirds. Mol. Ecol. 27:898–918.
201 Leducq J-B, Henault M, Charron G, Nielly-Thibault L, Terrat Y, Fiumera HL, Shapiro BJ, Landry CR.
202 2017. Mitochondrial recombination and introgression during speciation by hybridization. Mol.
203 Biol. Evol. 34:1947–1959.
204 Levsen N, Bergero R, Charlesworth D, Wolff K. 2016. Frequent, geographically structured
205 heteroplasmy in the mitochondria of a flowering plant, ribwort plantain (*Plantago lanceolata*).
206 Heredity. 117:1–7.
207 Librado P, Rozas J. 2009. DnaSP v5: A software for comprehensive analysis of DNA polymorphism
208 data. Bioinformatics. 25:1451–1452.
209 Lobley A, Sadowski MI, Jones DT. 2009. pGenTHREADER and pDomTHREADER: new methods for
210 improved protein fold recognition and superfamily discrimination. Bioinformatics 25:1761–1767.
211 Martin DP, Lemey P, Lott M, Moulton V, Posada D, Lefeuvre P. 2010. RDP3: A flexible and fast
212 computer program for analyzing recombination. Bioinformatics 26:2462–2463.
213 Martin DP, Murrell B, Golden M, Khoosal A, Muhire B. 2015. RDP4: Detection and analysis of
214 recombination patterns in virus genomes. Virus Evol. 1 (1):vev003.
215 Martin DP, Posada D, Crandall KA, Williamson C. 2005. A modified bootscan algorithm for automated
216 identification of recombinant sequences and recombination breakpoints. AIDS Res. Hum.
217 Retroviruses. 21:98–102.
218 Mastrantonio V, Porretta D, Urbanelli S, Crasta G, Nascetti G. 2016. Dynamics of mtDNA introgression
219 during species range expansion: insights from an experimental longitudinal study. Sci. Rep.
220 6:30355.
221 Mayer MP, Bukau B. 2005. Hsp70 chaperones: Cellular functions and molecular mechanism. Cell. Mol.
222 Life Sci. 62:670–684.
223 Miller MA, Pfeiffer W, Schwartz T. 2010. Creating the CIPRES Science Gateway for inference of large
224 phylogenetic trees. In: 2010 Gateway Computing Environments Workshop (GCE). IEEE. p. 1–8.
225 Morales HE, Pavlova A, Joseph L, Sunnucks P. 2015. Positive and purifying selection in mitochondrial
226 genomes of a bird with mitonuclear discordance. Mol. Ecol. 24:2820–2837.
227 Moustafa MZ, Hallock P. 2008. Observations of a Red Sea Fringing Coral Reef under Extreme
228 Environmental Conditions. 11th Int. Coral Reef Symp. Ft. Lauderdale, Florida:7–11.
229 Moustafa MZ, Moustafa MS, Moustafa ZD, Moustafa SE. 2014. Survival of high latitude fringing corals
230 in extreme temperatures: Red Sea oceanography. J. Sea Res. 88:144–151.
231 Nanninga GB, Saenz-Agudelo P, Manica A, Berumen ML. 2014. Environmental gradients predict the
232 genetic population structure of a coral reef fish in the Red Sea. Mol. Ecol. 23:591–602.

233 Padidam M, Sawyer S, Fauquet CM. 1999. Possible emergence of new geminiviruses by frequent
234 recombination. Virology. 265:218–225.
235 Pandolfi JM, Connolly SR, Marshall DJ, Cohen AL. 2011. Projecting coral reef futures under global
236 warming and ocean acidification. Science. 333:418–422.
237 Pavlova A, Amos JN, Joseph L, Loynes K, Austin JJ, Keogh JS, Stone GN, Nicholls JA, Sunnucks P.
238 2013. Perched at the mito-nuclear crossroads: divergent mitochondrial lineages correlate with
239 environment in the face of ongoing nuclear gene flow in an australian bird. Evolution. 67:3412–
240 3428.
241 Pellissier L, Leprieur F, Parravicini V, Cowman PF, Kulbicki M, Litsios G, Olsen SM, Wisz MS,
242 Bellwood DR, Mouillot D. 2014. Quaternary coral reef refugia preserved fish diversity. Science.
243 344:1016–1019.
244 Peris D, Arias A, Orlić S, Belloch C, Pérez-Través L, Querol A, Barrio E. 2017. Mitochondrial
245 introgression suggests extensive ancestral hybridization events among Saccharomyces species.
246 Mol. Phylogenet. Evol. 108:49–60.
247 Piganeau G, Gardner M, Eyre-Walker A. 2004. A broad survey of recombination in animal
248 mitochondria. Mol. Biol. Evol. 21:2319–2325.
249 Posada D, Crandall KA. 2001. Evaluation of methods for detecting recombination from DNA
250 sequences: Computer simulations. Proc. Natl. Acad. Sci. 98:13757–13762.
251 Raitsos DE, Pradhan Y, Brewin RJW, Stenchikov G, Hoteit I. 2013. Remote sensing the phytoplankton
252 seasonal succession of the red sea. PLoS One. 8:e64909.
253 Rambaut A, Drummond AJ. 2009. Tracer v 1.5. http://beast.bio.ed.ac.uk/Tracer.
254 Richards ZT, Hobbs JPA. 2015. Hybridisation on coral reefs and the conservation of evolutionary
255 novelty. Curr. Zool. 61:132–145.
256 Righton D, Kemp J, Ormond R. 1996. Biogeography community structure and diversity of Red Sea and
257 western Indian Ocean butterflyfishes. J. Mar. Biol. Assoc. United Kingdom 76:223–228.
258 Riginos C, Cunningham CW. 2004. Invited Review: Local adaptation and species segregation in two
259 mussel (*Mytilus edulis* × *Mytilus trossulus*) hybrid zones. Mol. Ecol. 14:381–400.
260 Roberts MB, Jones GP, McCormick MI, Munday PL, Neale S, Thorrold S, Robitzch VSN, Berumen
261 ML. 2016. Homogeneity of coral reef communities across 8 degrees of latitude in the Saudi
262 Arabian Red Sea. Mar. Pollut. Bull. 105:558–565.
263 Rohling EJ, Grant K, Hemleben C, Siddall M, Hoogakker BA, Bolshaw M, Kucera M. 2008. High rates
264 of sea-level rise during the last interglacial period. Nat. Geosci. 1:38–42.
265 Rohling EJ, Grant KM, Roberts AP, Larrasoaña JC. 2013. Paleoclimate variability in the mediterranean
266 and red sea regions during the last 500,000 years. Curr. Anthropol. 54:S183–S201.
267 Rokas A, Ladoukakis E, Zouros E. 2003. Animal mitochondrial DNA recombination revisited. Trends
268 Ecol. Evol. 18:411–417.
269 Saccone C, Lanave C, De Grassi A. 2006. Metazoan OXPHOS gene families: evolutionary forces at the
270 level of mitochondrial and nuclear genomes. Biochim. Biophys. Acta. 1757:1171–1178
271 Saenz-Agudelo P, Dibattista JD, Piatek MJ, Gaither MR, Harrison HB, Nanninga GB, Berumen ML.
272 2015. Seascape genetics along environmental gradients in the Arabian Peninsula: insights from
273 ddRAD sequencing of anemonefishes. Mol. Ecol. 24:6241–6255.
274 Salvi D, Pinho C, Harris DJ. 2017. Digging up the roots of an insular hotspot of genetic diversity:
275 decoupled mito-nuclear histories in the evolution of the Corsican-Sardinian endemic lizard
276 *Podarcis tiliguerta*. BMC Evol. Biol. 17:63.
277 Sawall Y, Al-Sofyani A, Banguera-Hinestroza E, Voolstra CR. 2014. Spatio-Temporal analyses of
278 symbiodinium physiology of the coral pocillopora verrucosa along large-scale nutrient and

temperature gradients in the red sea. PLoS One 9:e103179.
Sawall Y, Al-Sofyani A, Hohn S, Banguera-Hinestroza E, Voolstra CR, Wahl M. 2015. Extensive phenotypic plasticity of a Red Sea coral over a strong latitudinal temperature gradient suggests limited acclimatization potential to warming. Sci. Rep. 5:8940.
Scheer G, Pillai CSG. 1983. Report on the stony corals from the Red Sea. Zoologica 131:1–198.
Seutin G, White BN, Boag P. 1991. Preservation of avian blood and tissue samples for DNA analyses. Can. J. Zool. 69:89–90.
Shearer TL, Oppen MJH Van, Romano SL, G. Worheire. 2002. Slow mitochondria DNA sequence evolution in the Anthozoa (Cnidaria). Mol. Ecol. 11:2475–2487.
Siddall M, Rohling EJ, Almogi-Labin A, Hemleben C, Meischner D, Schmelzer I, Smeed D. 2003. Sea-level fluctuations during the last glacial cycle. Nature 423:853–858.
Siddall M, Smeed DA, Hemleben C, Rohling EJ, Schmelzer I, Peltier WR. 2004. Understanding the Red Sea response to sea level. Earth Planet. Sci. Lett. 225:421–434.
Smith DJ, Suggett DJ, Baker NR. 2005. Is photoinhibition of zooxanthellae photosynthesis the primary cause of thermal bleaching in corals? Glob. Chang. Biol. 11:1–11.
Smith JM. 1992. Analyzing the mosaic structure of genes. J. Mol. Evol. 34:126–129.
Stefani F, Benzoni F, Yang SY, Pichon M, Galli P, Chen CA. 2011. Comparison of morphological and genetic analyses reveals cryptic divergence and morphological plasticity in *Stylophora* (Cnidaria, Scleractinia). Coral Reefs. 30:1033–1049.
Stephens M, Donnelly P. 2003. A comparison of Bayesian methods for haplotype reconstruction from population genotype data. Am. J. Hum. Genet. 73:1162–1169.
Taviani M. 1998. Post-Miocene reef faunas of the Red Sea: glacio-eustatic controls. In: Sedimentation and tectonics in rift basins Red Sea-Gulf of Aden. Dordrecht: Springer Netherlands. p. 574–582.
Taylor SA, Larson EL, Harrison RG. 2015. Hybrid zones: windows on climate change. Trends Ecol. Evol. 30:398–406.
Toews, David P.L. Brelsford A. 2012. The biogeography of mitochondrial and nuclear discordance in animals. Mol. Ecol. 21:3907–3930.
Tsaousis AD, Martin DP, Ladoukakis ED, Posada D, Zouros E. 2005. Widespread recombination in published animal mtDNA sequences. Mol. Biol. Evol. 22:925–933.
Ujvari B, Dowton M, Madsen T. 2007. Mitochondrial DNA recombination in a free-ranging Australian lizard. Biol. Lett. 3:189–192.
Van Oppen MJH, McDonald BJ, Willis B, Miller DJ. 2001. The evolutionary history of the coral genus *Acropora* (Scleractinia, Cnidaria) based on a mitochondrial and a nuclear marker: reticulation, incomplete lineage sorting, or morphological convergence? Mol. Biol. Evol. 18:1315–1329.
Veron JEN. 1995. Corals in space and time: the biogeography and evolution of the Scleractinia. Cornell Univ. Press.
Veron JEN. 2002. New species described in corals of the world. Townsville: Australian Institute of Marine Science. 209 p.
Vollmer S V., Palumbi SR. 2002. Hybridization and the evolution of reef coral diversity. Science. 296:2023–2025.
White DJ, Wolff JN, Pierson M, Gemmell NJ. 2008. Revealing the hidden complexities of mtDNA inheritance. Mol. Ecol. 17:4925–4942.
Willis BL, van Oppen MJH, Miller DJ, Vollmer S V., Ayre DJ. 2006. The role of hybridization in the evolution of reef corals. Annu. Rev. Ecol. Evol. Syst. 37:489–517.
Wilton PR, Zaidi A, Makova K, Nielsen R. 2018. A population phylogenetic view of mitochondrial heteroplasmy. Genetics 208:1261–1274.

325 Wirth C, Brandt U, Hunte C, Zickermann V. 2016. Structure and function of mitochondrial complex I.
326 Biochim. Biophys. Acta - Bioenerg. 1857:902–914.
327 Wolff JN, Pichaud N, Camus MF, Côté G, Blier PU, Dowling DK. 2016. Evolutionary implications of
328 mitochondrial genetic variation: mitochondrial genetic effects on OXPHOS respiration and
329 mitochondrial quantity change with age and sex in fruit flies. J. Evol. Biol. 29:736–747.

Figure 1.

a)

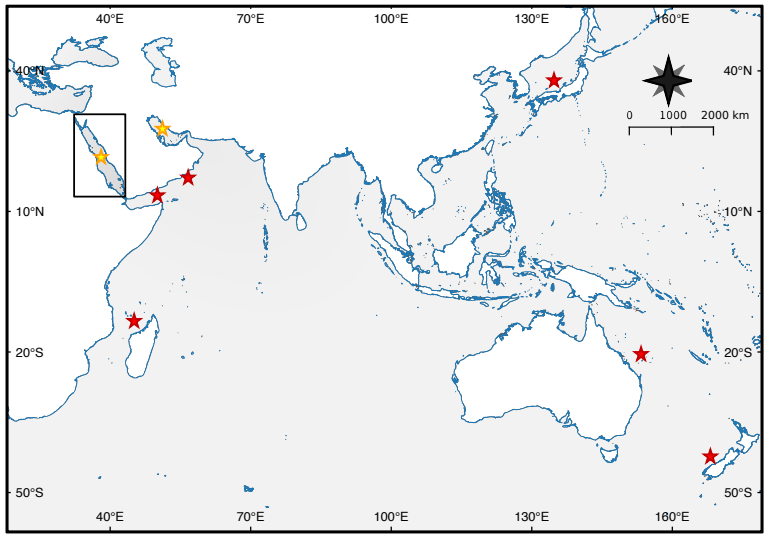

b)

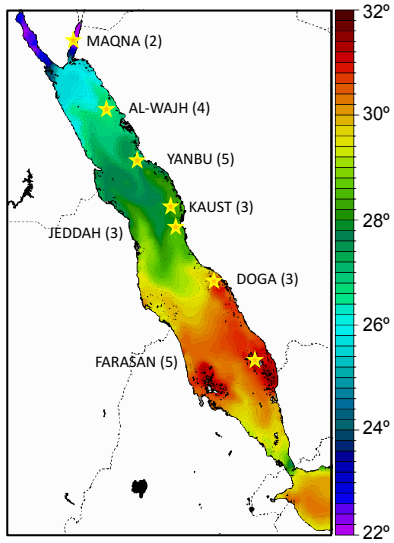

c)

Stylophora wellsi *Stylophora danae* *Stylophora subseriata* *Stylophora kuelhmanni* *Stylophora pistillata*

Figure 2.

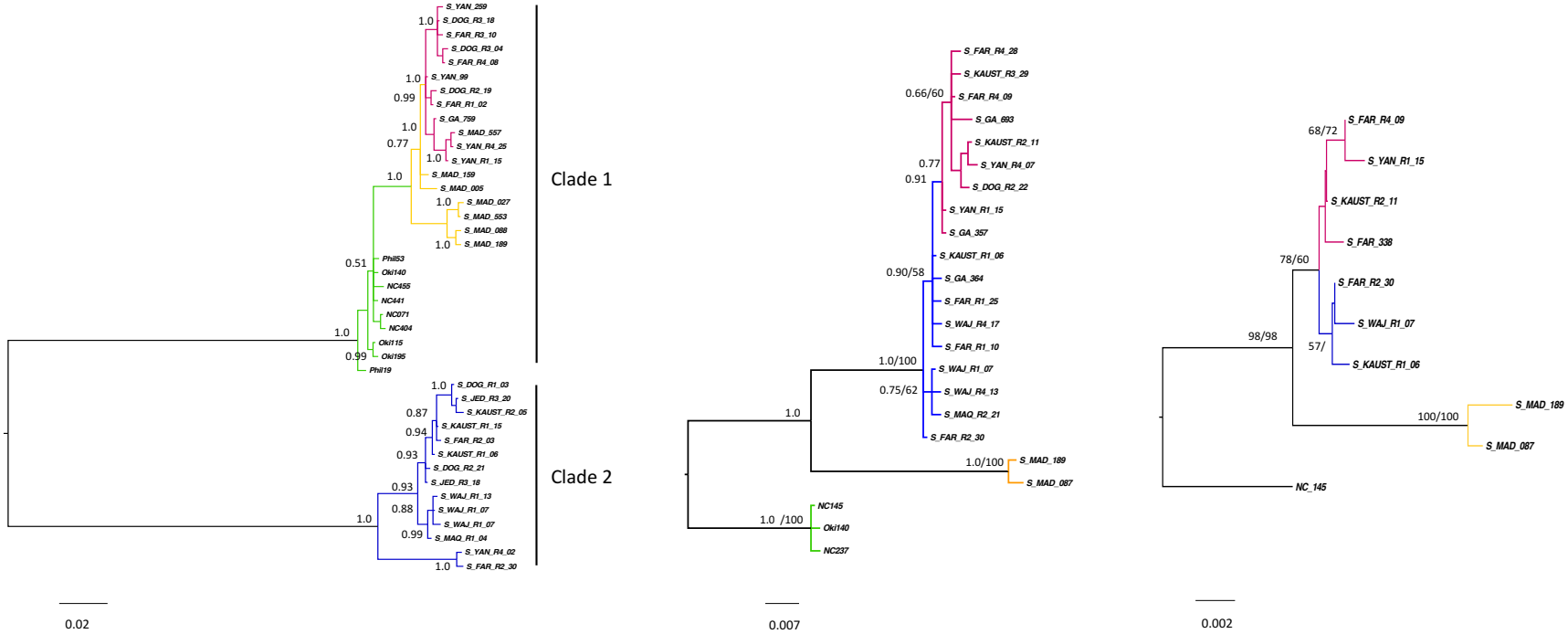
S_YAN_259
S_DOG_R3_18
S_FAR_R3_10
S_DOG_R3_04
S_FAR_R4_08
S_YAN_99
S_DOG_R2_19
S_FAR_R1_02
S_GA_759
S_MAD_557
S_YAN_R4_25
S_YAN_R1_15
S_MAD_159
S_MAD_005
S_MAD_027
S_MAD_553
S_MAD_088
S_MAD_189
Phil53
Oki140
NC455
NC441
NC071
NC404
Oki115
Oki195
Phil19
S_DOG_R1_03
S_JED_R3_20
S_KAUST_R2_05
S_KAUST_R1_15
S_FAR_R2_03
S_KAUST_R1_06
S_DOG_R2_21
S_JED_R3_18
S_WAJ_R1_13
S_WAJ_R1_07
S_WAJ_R1_07
S_MAQ_R1_04
S_YAN_R4_02
S_FAR_R2_30
Clade 1
Clade 2
0.02
S_FAR_R4_28
S_KAUST_R3_29
S_FAR_R4_09
S_GA_693
S_KAUST_R2_11
S_YAN_R4_07
S_DOG_R2_22
S_YAN_R1_15
S_GA_357
S_KAUST_R1_06
S_GA_364
S_FAR_R1_25
S_WAJ_R4_17
S_FAR_R1_10
S_WAJ_R1_07
S_WAJ_R4_13
S_MAQ_R2_21
S_FAR_R2_30
S_MAD_189
S_MAD_087
NC145
Oki140
NC237
0.007
S_FAR_R4_09
S_YAN_R1_15
S_KAUST_R2_11
S_FAR_338
S_FAR_R2_30
S_WAJ_R1_07
S_KAUST_R1_06
S_MAD_189
S_MAD_087
NC_145
0.002

a) b) c)

Figure 3.

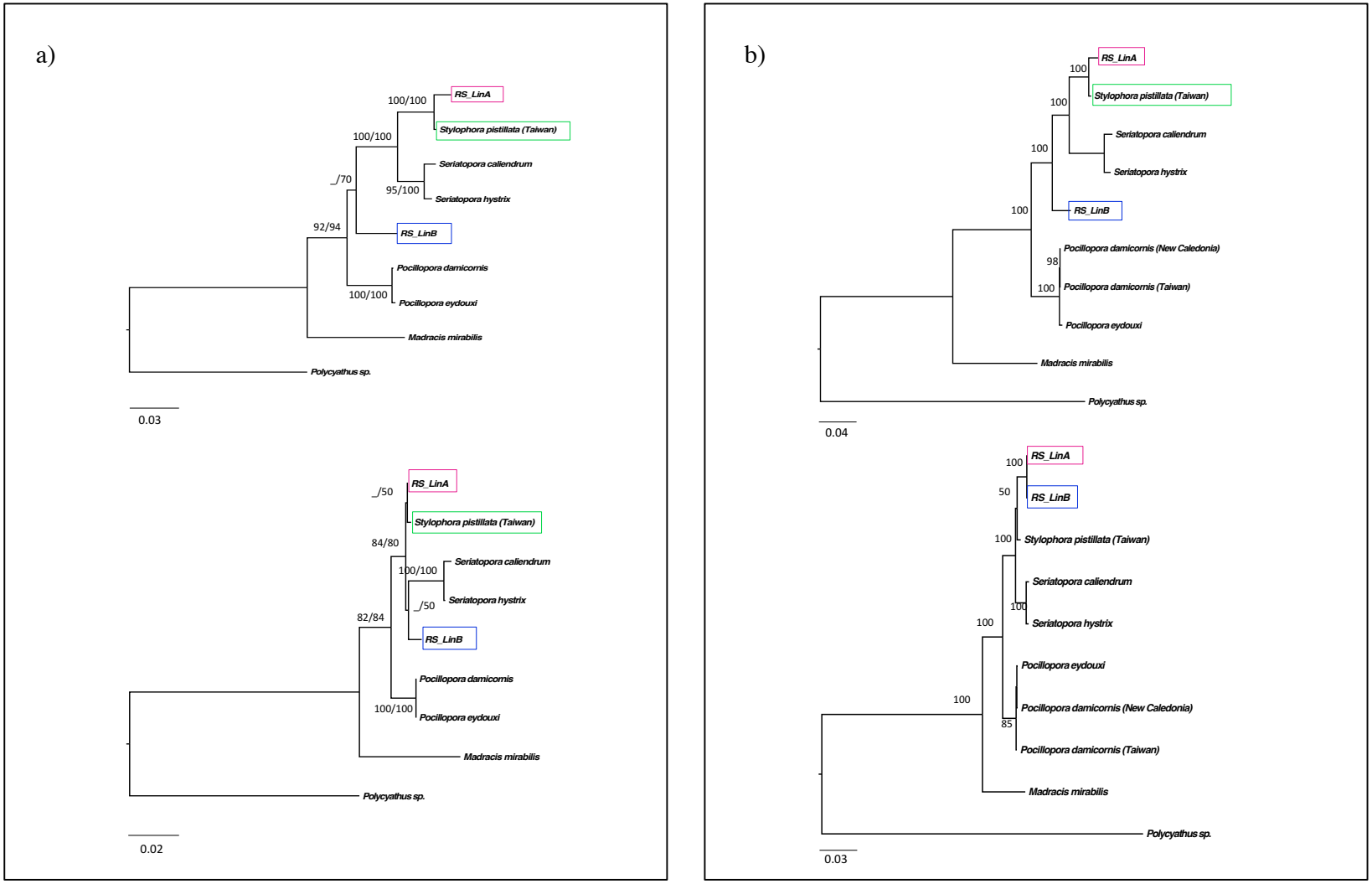
a)
100/100
RS_LinA
Stylophora pistillata (Taiwan)
100/100
Seriatopora caliendrum
_/70
95/100
Seriatopora hystrix
92/94
RS_LinB
Pocillopora damicornis
100/100
Pocillopora eydouxi
Madracis mirabilis
Polycyathus sp.
0.03
_/50
RS_LinA
Stylophora pistillata (Taiwan)
84/80
100/100
Seriatopora caliendrum
_/50
Seriatopora hystrix
82/84
RS_LinB
Pocillopora damicornis
100/100
Pocillopora eydouxi
Madracis mirabilis
Polycyathus sp.
0.02
b)
100
RS_LinA
100
Stylophora pistillata (Taiwan)
100
Seriatopora caliendrum
Seriatopora hystrix
100
RS_LinB
98
Pocillopora damicornis (New Caledonia)
100
Pocillopora damicornis (Taiwan)
Pocillopora eydouxi
Madracis mirabilis
Polycyathus sp.
0.04
100
RS_LinA
50
RS_LinB
100
Stylophora pistillata (Taiwan)
Seriatopora caliendrum
100
Seriatopora hystrix
100
Pocillopora eydouxi
100
Pocillopora damicornis (New Caledonia)
85
Pocillopora damicornis (Taiwan)
Madracis mirabilis
Polycyathus sp.
0.03

Figure 4.

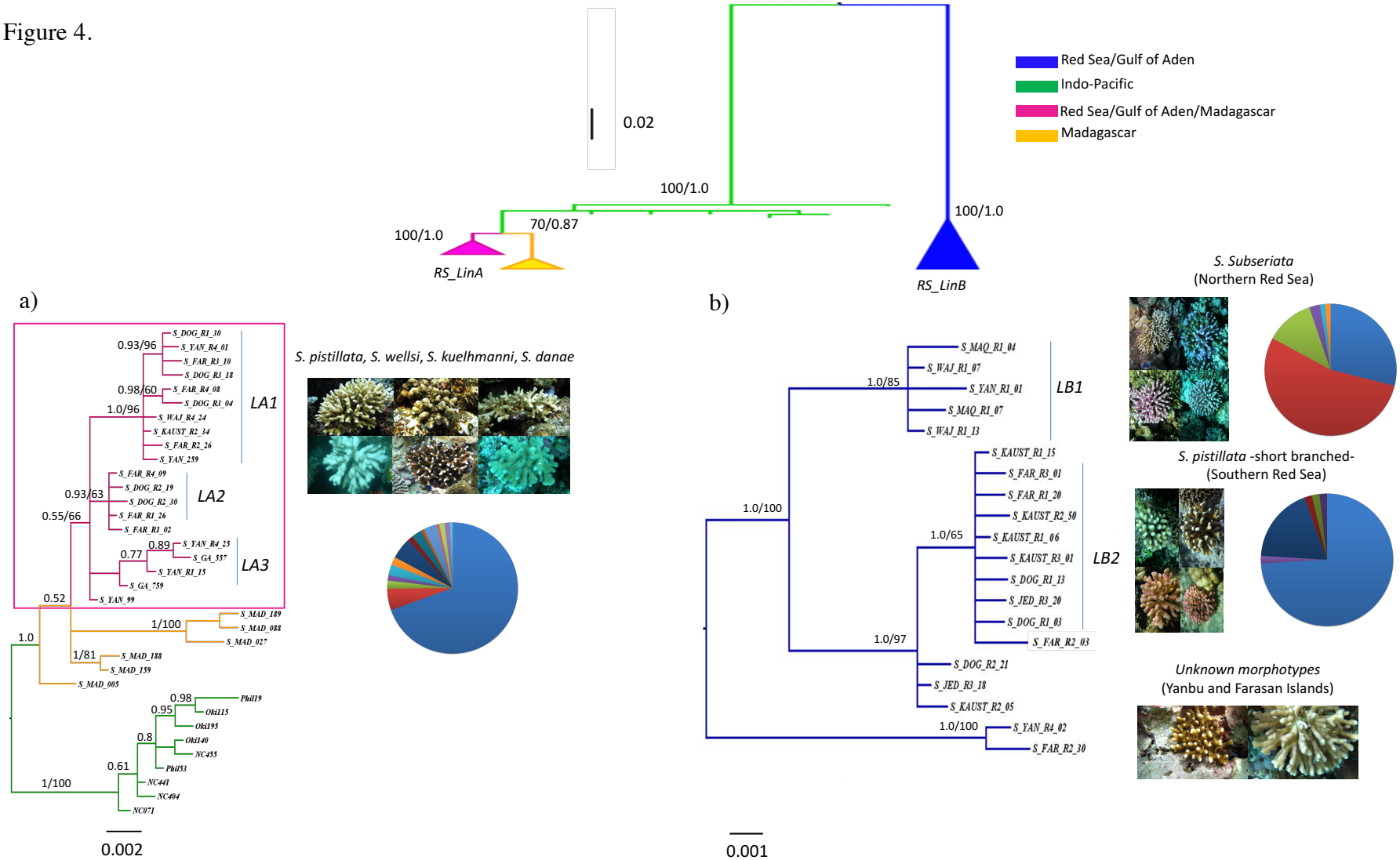

Symbiodinium types

A1	C160	A1-C160	C116	C161	C1*	A1-C1*	A1-sp	A1-C3
F	C162	A1-D	A1-C41	A1-B	A1-C1	A1-C19	C1*- sp.	

Figure 5.

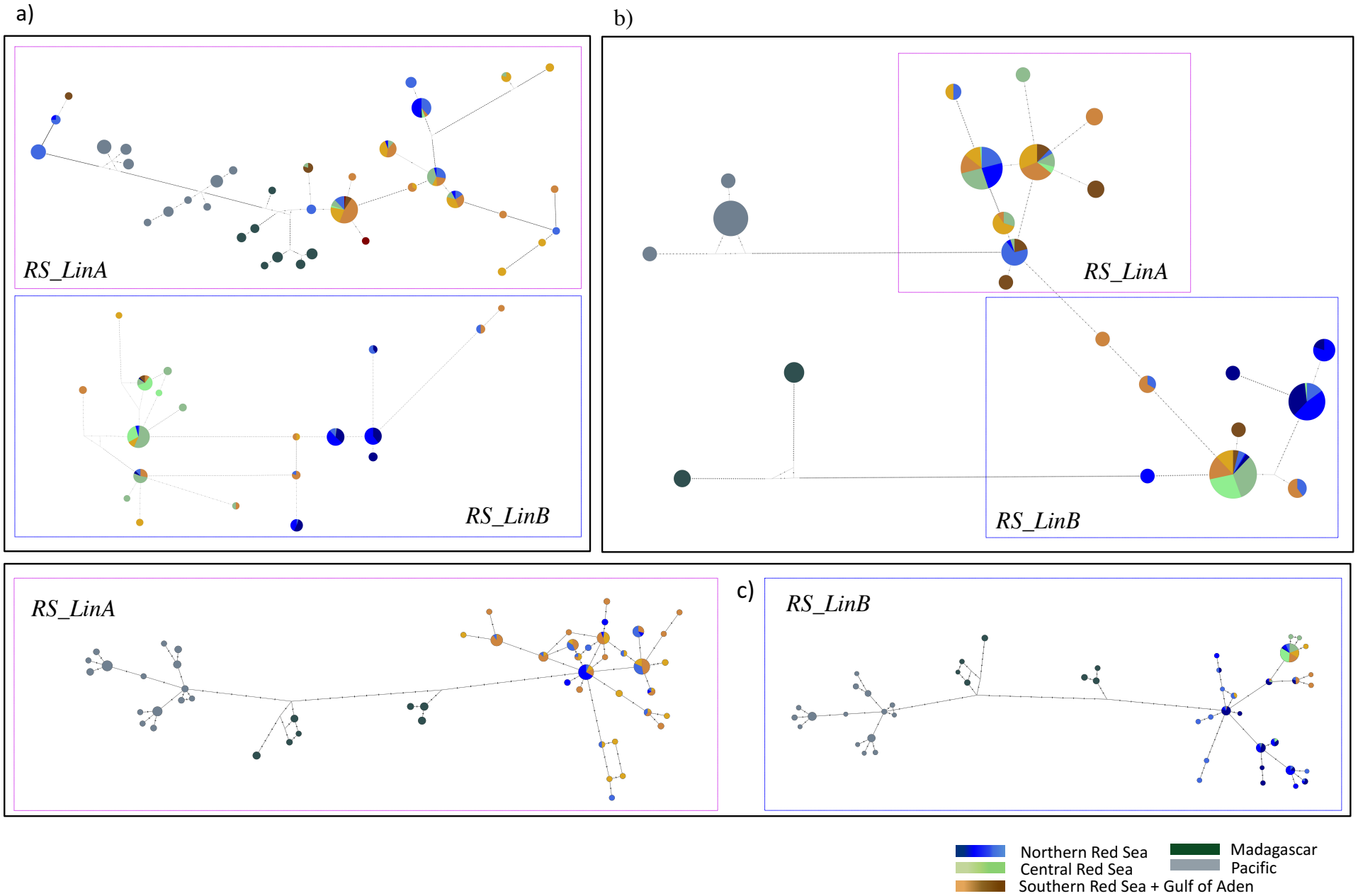
a)
RS_LinA
RS_LinB
b)
RS_LinA
RS_LinB
c)
RS_LinA
RS_LinB
Northern Red Sea
Central Red Sea
Southern Red Sea + Gulf of Aden
Madagascar
Pacific

Supplementary Figure *S1*.

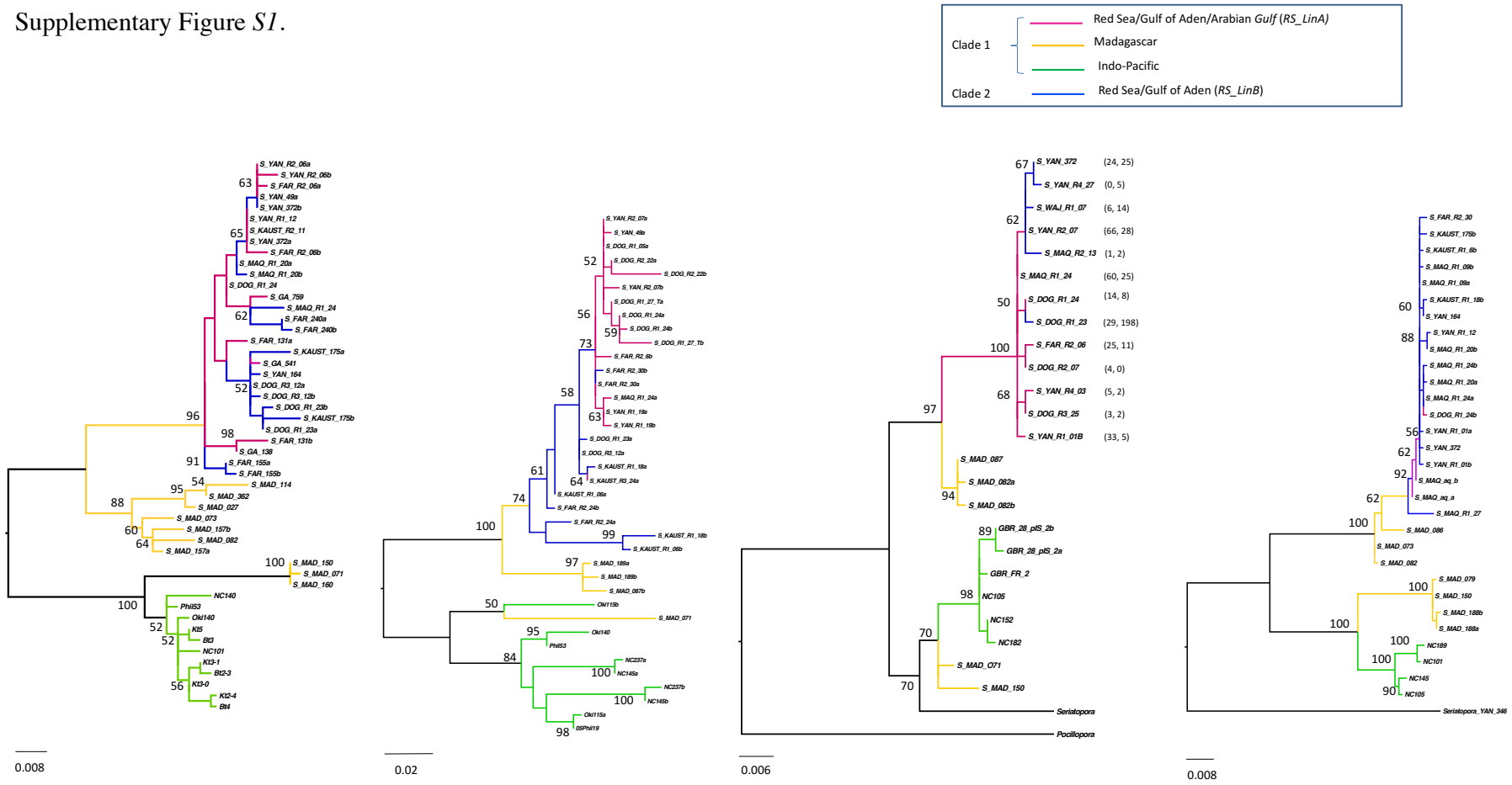

Supplementary Figure *S2a*.

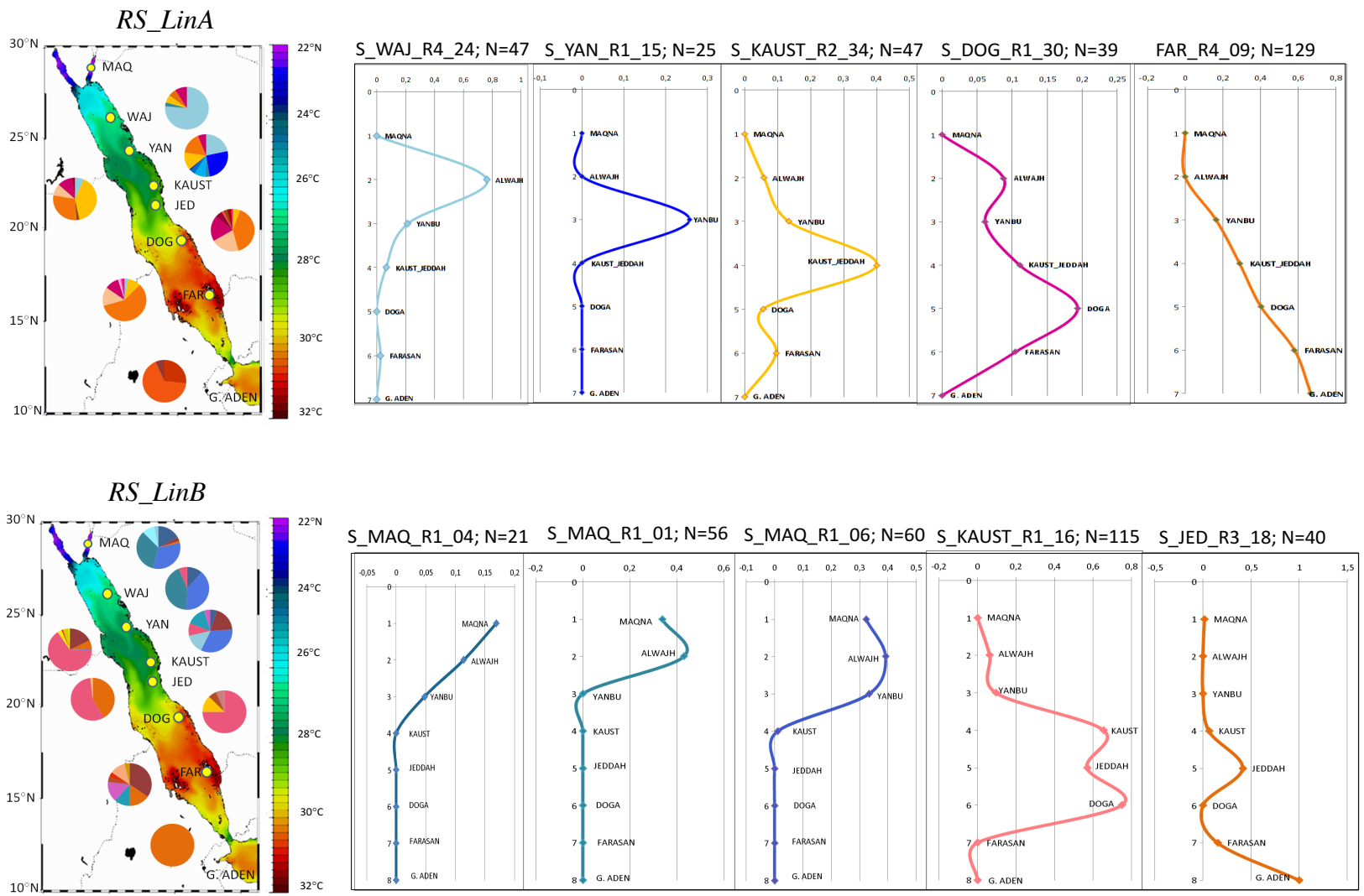

Supplementary Figure *S2b*.

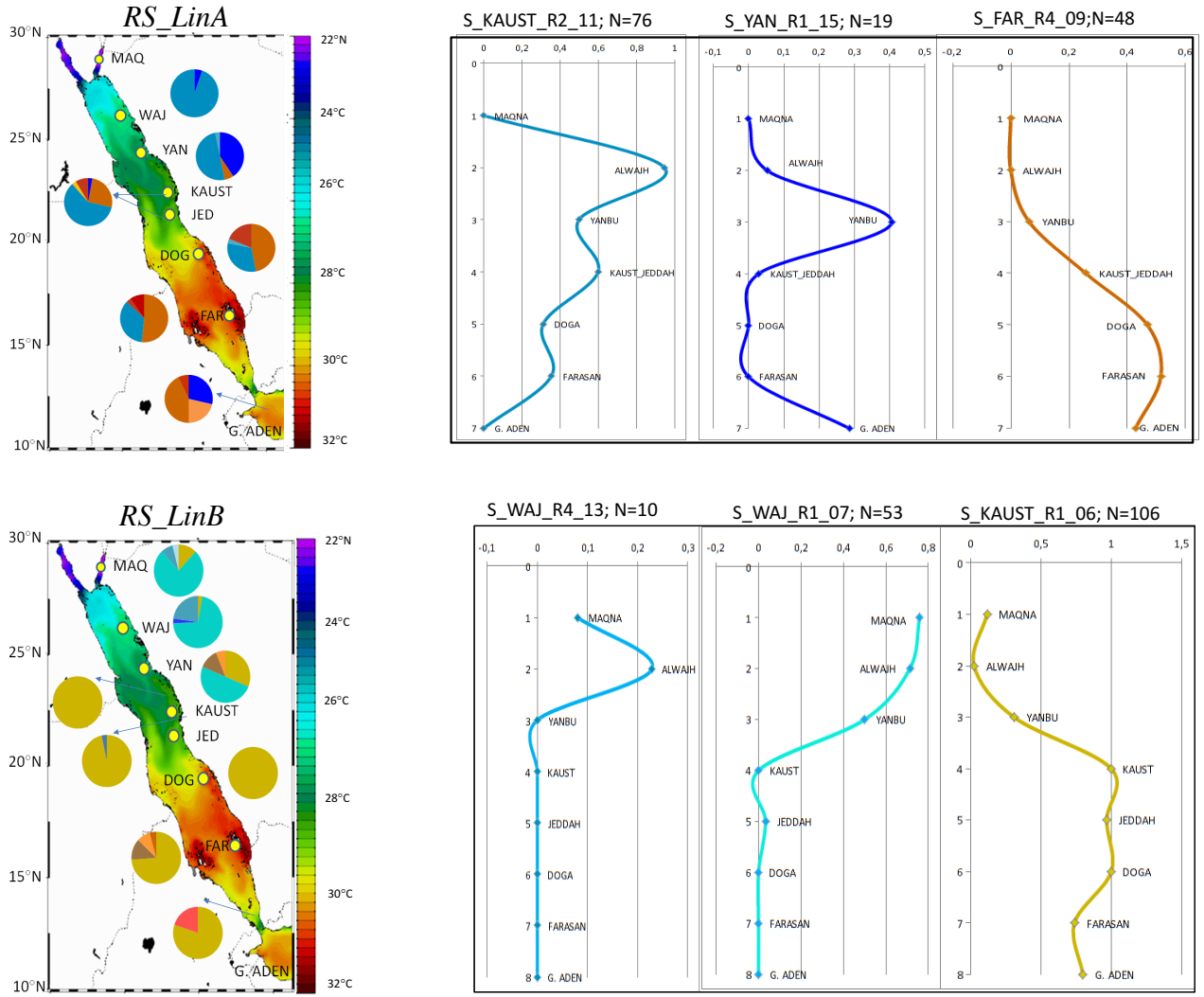

Supplementary Figure *S2c*.

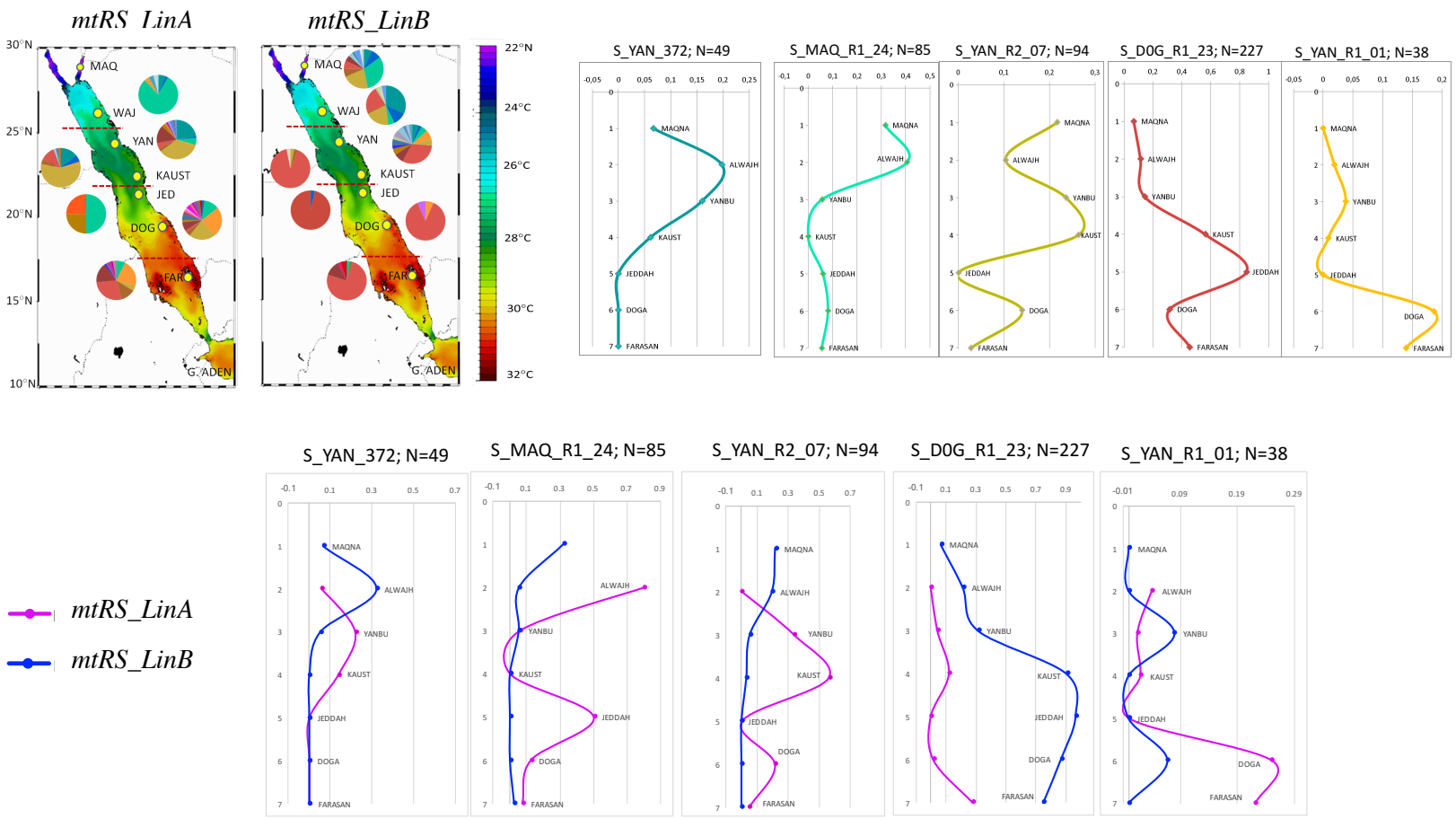

Supplementary Figure *S3*.

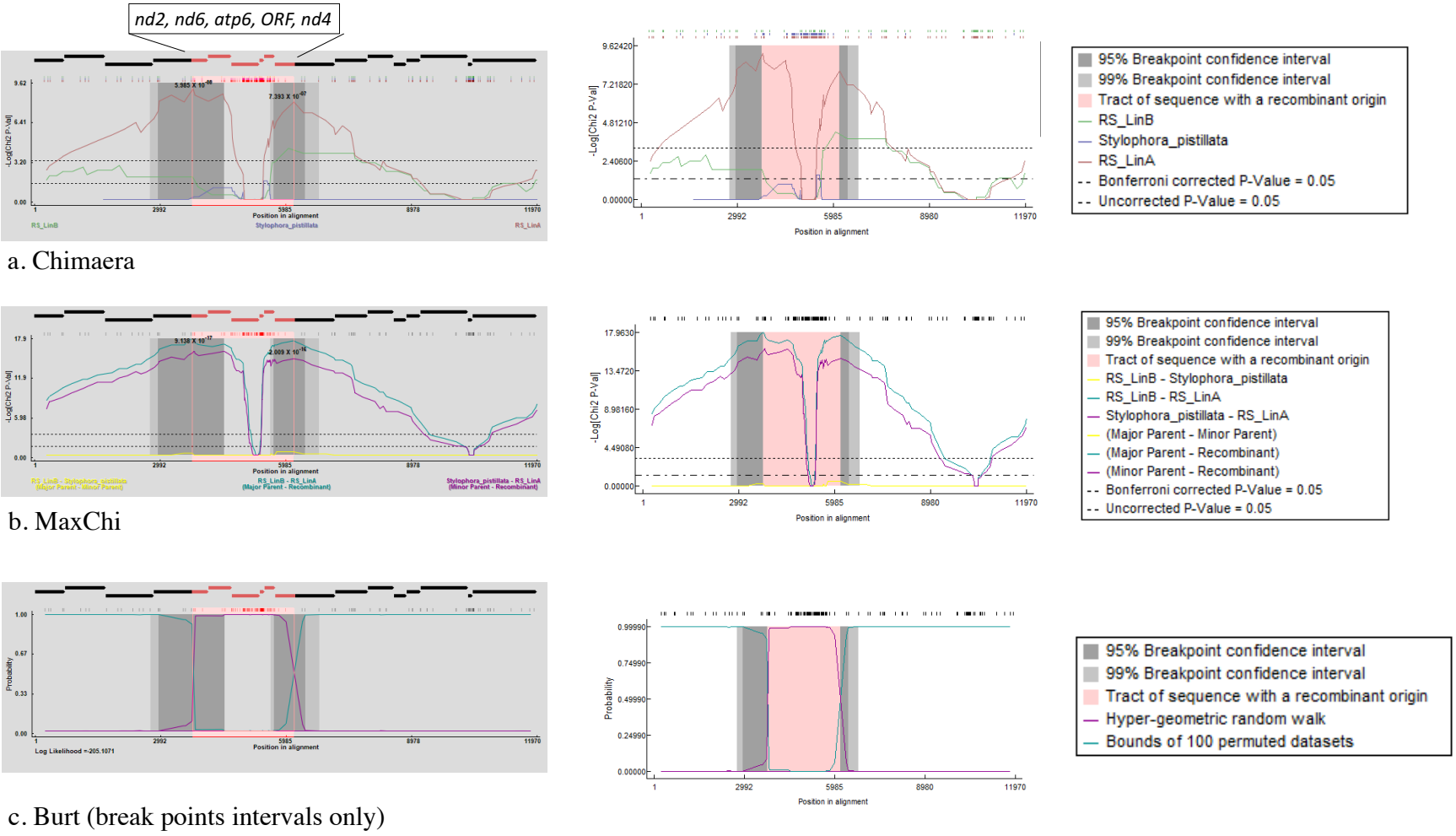

a. Chimaera

b. MaxChi

c. Burt (break points intervals only)